NeuroImage 295 (2024) 120636

Contents lists available at ScienceDirect

NeuroImage

journal homepage: www.elsevier.com/locate/ynimg

# Brain health in diverse settings: How age, demographics and cognition shape brain function

Hernan Hernandez [a,1], Sandra Baez [b,c,1], Vicente Medel [a], Sebastian Moguilner [a,d], Jhosmary Cuadros [a,e,f], Hernando Santamaria-Garcia [g,h], Enzo Tagliazucchi [a,i], Pedro A. Valdes-Sosa [k,l], Francisco Lopera [m], John Fredy OchoaGómez [m], Alfredis González-Hernández [n], Jasmin Bonilla-Santos [o], Rodrigo A. Gonzalez-Montealegre [p], Tuba Aktürk [ap], Ebru Yıldırım [ap], Renato Anghinah [q,r], Agustina Legaz [a,s,t,u], Sol Fittipaldi [a,c,ab], Görsev G. Yener [v,w,x], Javier Escudero [y], Claudio Babiloni [z,aa], Susanna Lopez [z], Robert Whelan [c,ac], Alberto A Fernández Lucas [ac], Adolfo M. García [c,ad,ae], David Huepe [af], Gaetano Di Caterina [ag], Marcio Soto-Añari [ah], Agustina Birba [a], Agustin Sainz-Ballesteros [a], Carlos Coronel [a,c,ai], Eduar Herrera [aj], Daniel Abasolo [ak], Kerry Kilborn [al], Nicolás Rubido [am], Ruaridh Clark [an], Ruben Herzog [a,ao], Deniz Yerlikaya [ap], Bahar Güntekin [aq,ar], Mario A. Parra [as], Pavel Prado [j], Agustin Ibanez [a,at,au,av,*]

[a] Latin American Brain Health Institute, Universidad Adolfo Ibañez, Santiago de Chile, Chile
[b] Universidad de los Andes, Bogota, Colombia
[c] Global Brain Health Institute (GBHI), University of California, San Francisco, US Trinity College Dublin, Dublin, Ireland
[d] Harvard Medical School, Boston, MA, USA
[e] Advanced Center for Electrical and Electronic Engineering, Universidad Técnica Federico Santa María, Valparaíso 2390123, Chile
[f] Grupo de Bioingeniería, Decanato de Investigación, Universidad Nacional Experimental del Táchira, San Cristóbal 5001, Venezuela
[g] Pontificia Universidad Javeriana (PhD Program in Neuroscience) Bogotá, San Ignacio, Colombia
[h] Center of Memory and Cognition Intellectus, Hospital Universitario San Ignacio Bogotá, San Ignacio, Colombia
[i] University of Buenos Aires, Argentina
[j] Escuela de Fonoaudiología, Facultad de Odontología y Ciencias de la Rehabilitación, Universidad San Sebastián, Santiago, Chile
[k] The Clinical Hospital of Chengdu Brain Sciences, University of Electronic Sciences Technology of China, Chengdu, China
[l] Cuban Neuroscience Center, La Habana, Cuba
[m] Grupo de Neurociencias de Antioquia, University of Antioquia, Medellín, Colombia
[n] Master programme of Clinical Neuropsychology, Universidad Surcolombiana, Neiva Huila, Colombia
[o] Department of Psychology, Universidad Cooperativa de Colombia, Colombia
[p] Neurocognition and Psychophysiology Laboratory, Universidad Surcolombiana, Neiva Huila, Colombia
[q] Reference Center of Behavioural Disturbances and Dementia, School of Medicine, University of Sao Paulo, Sao Paulo, Brazil
[r] Traumatic Brain Injury Cognitive Rehabilitation Out-Patient Center, University of Sao Paulo, Sao Paulo, Brazil
[s] Cognitive Neuroscience Center, Universidad de San Andrés, Buenos Aires, Argentina
[t] National Scientific and Technical Research Council (CONICET), Buenos Aires, Argentina
[u] Facultad de Psicología, Universidad Nacional de Córdoba, Córdoba, Argentina
[v] Faculty of Medicine, Izmir University of Economics, 35330, Izmir, Turkey
[w] Brain Dynamics Multidisciplinary Research Center, Dokuz Eylul University, Izmir, Turkey
[x] Izmir Biomedicine and Genome Center, Izmir, Turkey
[y] School of Engineering, Institute for Imaging, Data and Communications, University of Edinburgh, Scotland, UK
[z] Department of Physiology and Pharmacology "V. Erspamer", Sapienza University of Rome, Rome, Italy
[aa] Hospital San Raffaele Cassino, Cassino, (FR), Italy
[ab] School of Psychology, Trinity College Dublin, Dublin, Ireland
[ac] Department of Legal Medicine, Psychiatry and Pathology at the Complutense University of Madrid, Madrid, Spain
[ad] Cognitive Neuroscience Center, Universidad de San Andréss, Buenos Aires, Argentina
[ae] Departamento de Lingüística y Literatura, Facultad de Humanidades, Universidad de Santiago de Chile, Santiago, Chile
[af] Center for Social and Cognitive Neuroscience (CSCN), School of Psychology, Universidad Adolfo Ibáñez
[ag] Department of Electronic and Electrical Engineering, University of Strathclyde, Glasgow, UK
[ah] Universidad Católica San Pablo, Arequipa, Peru

* Corresponding author.
*E-mail address:* agustin.ibanez@gbhi.org (A. Ibanez).

https://doi.org/10.1016/j.neuroimage.2024.120636
Received 8 February 2024; Received in revised form 17 April 2024; Accepted 4 May 2024
Available online 21 May 2024

[ai] Centro Interdisciplinario de Neurociencia de Valparaíso (CINV), Universidad de Valparaíso, Valparaíso, Chile
[aj] Departamento de Estudios Psicológicos, Universidad ICESI, Cali, Colombia
[ak] Centre for Biomedical Engineering, School of Mechanical Engineering Sciences, Faculty of Engineering and Physical Sciences, University of Surrey, Guildford GU2 7XH, UK
[al] School of Psychology, University of Glasgow, Glasgow, Scotland, UK
[am] Institute for Complex Systems and Mathematical Biology, University of Aberdeen, Aberdeen, AB24 3UE, UK
[an] Centre for Signal and Image Processing, Department of Electronic and Electrical Engineering, University of Strathclyde, UK
[ao] Sorbonne Université, Institut du Cerveau - Paris Brain Institute - ICM, Inserm, CNRS, Paris 75013, France
[ap] Department of Neurosciences, Health Sciences Institute, Dokuz Eylül University, Izmir, Turkey
[aq] Health Sciences and Technology Research Institute (SABITA), Istanbul Medipol University, Istanbul, Turkey
[ar] Department of Biophysics, School of Medicine, Istanbul Medipol University, Turkey
[as] Department of Psychological Sciences and Health, University of Strathclyde, United Kingdom and Associate Researcher of the Latin American Brain Health Institute (BrainLat), Universidad Adolfo Ibáñez, Santiago, Chile
[at] Global Brain Health Institute, University of California San Francisco, San Francisco, CA, USA
[au] Cognitive Neuroscience Center, Universidad de San Andrés and Consejo Nacional de Investigaciones Científicas y Técnicas, Buenos Aires, Argentina
[av] Trinity College Dublin, The University of Dublin, Dublin, Ireland

ARTICLE INFO

*Keywords:*
Age
Cognition
Education
Individual differences
Sex
Brain dynamics

ABSTRACT

Diversity in brain health is influenced by individual differences in demographics and cognition. However, most studies on brain health and diseases have typically controlled for these factors rather than explored their potential to predict brain signals. Here, we assessed the role of individual differences in demographics (age, sex, and education; $n = 1298$) and cognition ($n = 725$) as predictors of different metrics usually used in case-control studies. These included power spectrum and aperiodic (1/f slope, knee, offset) metrics, as well as complexity (fractal dimension estimation, permutation entropy, Wiener entropy, spectral structure variability) and connectivity (graph-theoretic mutual information, conditional mutual information, organizational information) from the source space resting-state EEG activity in a diverse sample from the global south and north populations. Brain-phenotype models were computed using EEG metrics reflecting local activity (power spectrum and aperiodic components) and brain dynamics and interactions (complexity and graph-theoretic measures). Electrophysiological brain dynamics were modulated by individual differences despite the varied methods of data acquisition and assessments across multiple centers, indicating that results were unlikely to be accounted for by methodological discrepancies. Variations in brain signals were mainly influenced by age and cognition, while education and sex exhibited less importance. Power spectrum activity and graph-theoretic measures were the most sensitive in capturing individual differences. Older age, poorer cognition, and being male were associated with reduced alpha power, whereas older age and less education were associated with reduced network integration and segregation. Findings suggest that basic individual differences impact core metrics of brain function that are used in standard case-control studies. Considering individual variability and diversity in global settings would contribute to a more tailored understanding of brain function.

## 1. Introduction

Individual differences encompass variations observed within a population in relation to a specific trait, including socio-demographic characteristics, as well as psychological and cognitive factors (Senner et al., 1814). Individual differences in age (Cole et al., 2018; Bethlehem et al., 2022), sex (Dotson and Duarte, 2020; Tang et al., 2022; Allouh et al., 2020), education (Garcia et al., 2018; Members et al., 2010), and cognition (Valsdóttir et al., 2022; Heger et al., 2021) are currently assumed to play a relevant role in brain function, driving diversity in brain health (Santamaria-Garcia et al., 2023; Greene et al., 2022; Aranda et al., 2021; Livingston et al., 2020; Holmes and Patrick, 2018). Diversity in the context of brain health refers to wide range of factors related to populations in terms of race, ethnicity, gender, age, socioeconomic status, cognitive variability, geographical location, genetic background, and health status, among others (Santamaria-Garcia et al., 2023; Fittipaldi et al., 2023; Matshabane, 2021). Diversity impacts healthy aging (Santamaria-Garcia et al., 2023), psychiatric conditions (Holmes and Patrick, 2018; Resende et al., 2019), and neurodegeneration (Ibanez et al., 2023; Walsh et al., 2022). However, these effects are not universally shared across regions (Santamaria-Garcia et al., 2023; Greene et al., 2022; Holmes and Patrick, 2018; Alladi and Hachinski, 2018), and may not generalize to more diverse, underrepresented populations in brain health research (Dotson and Duarte, 2020; Santamaria-Garcia et al., 2023; Baez et al., 2023).

Recent findings underscore the significance of individual differences in demographic predictors, showing that brain-phenotype models primarily reflect these variables rather than the intended cognitive domains, particularly in non-stereotypical populations (Greene et al., 2022). Notwithstanding, most studies on brain health and aging (Jawinski et al., 2022; Yan et al., 2015), psychiatry (Wolfers et al., 2020; Elad et al., 2021), and neurodegeneration (Pinaya et al., 2021; Verdi et al., 2022) have typically controlled for these variables rather than investigating their impact on brain-phenotype associations. Incorporating the role of individual differences, including demographics and cognition, in functional brain dynamics across large, heterogeneous and underrepresented populations may provide a direct pathway to a better understanding of the impact of diversity on brain health.

The study of demographics and cognition as predictors of brain signals has predominantly relied on MRI or fMRI (Bethlehem et al., 2022; Elad et al., 2021; Di Biase et al., 2023; Rutherford et al., 2022; Habes et al., 2021; Rosenberg et al., 2020). A limited number of reports have incorporated MEG (Dimitriadis, 2022; Stier et al., 2023), and only one has used EEG (Hill et al., 2022). Age has consistently emerged as the most frequently studied demographic factor for predicting structural and functional changes in the human brain, spanning from post-conception to aging, both in healthy individuals (Bethlehem et al., 2022; Di Biase et al., 2023; Rutherford et al., 2022; Dimitriadis, 2022; Stier et al., 2023) and in patients with psychiatric (Elad et al., 2021) or neurodegenerative conditions (Bethlehem et al., 2022). While sex is considered a predictor of brain changes across the lifespan (Bethlehem et al., 2022; Rutherford et al., 2022; Stier et al., 2023), the impacts of other relevant variables, such as education and cognition (Rosenberg

[1] Equal contribution.

et al., 2020; Greene et al., 2020; Garo-Pascual et al., 2023; Cesnaite et al., 2023), have been less explored. Both education (Gordon et al., 2008; Jokinen et al., 2016) and cognition (Habes et al., 2021) have been associated with white matter changes and increased functional connectivity (Franzmeier et al., 2071a, 2017b). However, while previous studies have investigated how demographic and cognitive factors influence brain signals, few have explored the effects of age, sex, education, and cognition simultaneously. This research gap highlights the need for studies that comprehensively explore the interplay between demographic factors, cognitive abilities, and brain signals using various imaging modalities, including EEG. These advancements would represent a crucial step towards robustly quantifying individual variations and their associations with signatures of brain functional organization or reorganization, especially in global research settings exhibiting larger heterogeneity.

Given the limited accessibility of neuroimaging or MEG measures on a large scale, more cost-effective and scalable techniques, such as EEG, may be better suited for studying individual differences in global settings. Neuroimaging measures often exhibit poor reliability and low power, requiring thousands of participants to demonstrate brain-phenotype associations (Marek et al., 2022). The non-invasiveness, scalability, availability, temporal resolution, and low cost of EEG make it an attractive approach to meet this need (Prado et al., 2022). Although many studies have explored the association of EEG metrics with demographics and cognition, only one study have used these variables to predict EEG signals (Hill et al., 2022). Studies have identified age-related EEG changes in resting and task performance (Valsdóttir et al., 2022; Cesnaite et al., 2023; Al Zoubi et al., 2018; Carrier et al., 2001; Hinault et al., 2023; Javaid et al., 2022; Merkin et al., 2023; Meunier et al., 2009; Murty et al., 2020; Smith et al., 2023; Smits et al., 2016; Song et al., 2014; Stacey et al., 2021; Trammell et al., 2017; Trondle et al., 2023; Valdes-Sosa et al., 2021; Voytek et al., 2015; Zappasodi et al., 2015), including alpha amplitude, as well as slowdown and increases in global power (Cesnaite et al., 2023; Trondle et al., 2023; Gaal et al., 2010), topographic reorganization in delta and theta frequencies (Ishii et al., 2017; Rossini et al., 2007), and attenuated spontaneous gamma oscillations (Murty et al., 2020). Complexity changes across the lifespan with increases during young adulthood and decreases in the elderly population (Zappasodi et al., 2015) have been reported. Age also induces changes in the aperiodic components (Hinault et al., 2023; Trondle et al., 2023; Donoghue et al., 2020) and reductions in global and local efficiencies as well as small-worldness (Javaid et al., 2022; Meunier et al., 2009; Achard and Bullmore, 2007; Onoda and Yamaguchi, 2013). The association of sex and EEG metrics is less conclusive (Carrier et al., 2001; Pravitha et al., 2005; Miraglia et al., 2015). Conversely, the link between cognition and EEG signals is well-established, with theta (Finnigan and Robertson, 2011) and alpha (Lejko et al., 2020) associations, decrease in random and spontaneous neural activity (Smith et al., 2023; Ouyang et al., 2020; Pei et al., 2023), increased complexity (Smith et al., 2023; Ouyang et al., 2020; Pei et al., 2023), higher network integration (Finnigan and Robertson, 2011; Bullmore and Sporns, 2009; Iinuma et al., 2022; McBride et al., 2014), and small-world properties (Liao et al., 2017). The association between education and EEG metrics has been rarely reported, with limited evidence (Wilkinson et al., 2023). Furthermore, although EEG studies have improved preprocessing pipelines (Prado et al., 2022; Bigdely-Shamlo et al., 2015; Ballesteros et al., 2023; Prado et al., 2023), several methodological caveats continue to hinder their effective use in large-scale studies. The recording heterogeneity, different layouts of electrodes and amplifiers, lack of harmonization, disparate processing pipelines, and small sample sizes, have restricted broader application of EEG (Prado et al., 2022; Jovicich et al., 2019). Thus, there is a critical need for studies in large and diverse samples using demographic or cognitive variables to predict brain signals via EEG while addressing its sources of heterogeneity.

To address these gaps, this study explored EEG data from a large and diverse sample of healthy participants under resting-state conditions from regions in the global south (Argentina, Brazil, Colombia, Chile, Cuba) and the global north (Ireland, Italy, Turkey, United Kingdom). We aimed to validate the relationships between demographic (i.e., age, sex, and education; $n = 1298$) and cognitive factors ($n = 725$) with the EEG metrics across a diverse, heterogeneous, and global dataset. Additionally, we investigated their utility in predicting significant changes in brain function, even in the presence of large heterogeneity. We computed brain-phenotype models of local activity [i.e., power spectrum and aperiodic components (Hill et al., 2022; Varela et al., 2001)], and brain dynamics and interactions [i.e., complexity, and graph-theoretic measures (Bullmore and Sporns, 2009; Iinuma et al., 2022)]. We selected these metrics based on their established relevance to demographic factors, their potential implications for understanding brain function, and their frequent use across different studies. These metrics have shown associations with the features assessed in our study, namely age (Cesnaite et al., 2023; Stacey et al., 2021; Gaal et al., 2010), sex (Carrier et al., 2001; Pravitha et al., 2005; Miraglia et al., 2015), education (Wilkinson et al., 2023), and cognition (Finnigan and Robertson, 2011; Bullmore and Sporns, 2009; Iinuma et al., 2022; McBride et al., 2014). Power spectrum metrics reveal dominant rhythms linked with cognitive processes and brain states (Klimesch, 1999), while spectral EEG metrics interpret non-rhythmic brain activity relevant to aging and cognition (Donoghue et al., 2020). Complexity metrics provide insights into the dynamics of different brain regions and their interactions, potentially serving as biomarkers for brain health disorders (Tononi et al., 1994; Lau et al., 2022). Graph-theoretic metrics illuminate functional connectivity patterns and network organization (Bullmore and Sporns, 2009). These metrics served as outcomes to evaluate the predictive value of each demographic and cognitive variable under two conditions: (a) when it served as the most robust predictor within the model, and (b) when another variable was considered the best predictor. Additionally, we explored the source space for each of brain-phenotype models.

We hypothesized that despite the sample diversity and heterogeneity, a subset of the demographic and cognitive variables would significantly predict each EEG metric. We expected that age (Rosenberg et al., 2020; Hill et al., 2022; Carrier et al., 2001; Javaid et al., 2022; Merkin et al., 2023; Meunier et al., 2009; Murty et al., 2020; Smith et al., 2023; Smits et al., 2016) and cognition (Carrier et al., 2001; Hinault et al., 2023; Smits et al., 2016; Song et al., 2014) would emerge as the most robust predictors of EEG metrics. We also anticipated that the combined effects of these two factors would result in models explaining a high proportion of variance of EEG measures. The influence of sex (Merkin et al., 2023; Stacey et al., 2021; Trammell et al., 2017) and education (Trondle et al., 2023) would be weaker. Our results suggest that individual differences in diverse settings impact core metrics of brain function that are used in standard case-control studies. The role of individual differences and diversity in contributing to brain function needs to be addressed more systematically in global contexts.

## 2. Materials and methods

### 2.1. Participants

This multicentric study involved 1298 healthy adult participants (age: mean = 46.60, SD = 20.76, range 18–91 years;; years of formal education: mean = 13.77, SD = 4.38; sex: $M = 597$, $F = 701$) representing diverse populations (Fig. 1A) from the global south (Argentina, Brazil, Colombia, Chile, Cuba) and the global north (Ireland, Italy, Turkey, United Kingdom). Demographic characteristics and sample sizes for each country are provided in Table 1. Participants had no history of psychiatric and/or neurological disorders, alcohol/drug abuse, significant visual and/or auditory impairments. Furthermore, participants were not using any ferromagnetic implant. No participant reported subjective cognitive complaints or functional impairments. Data on the

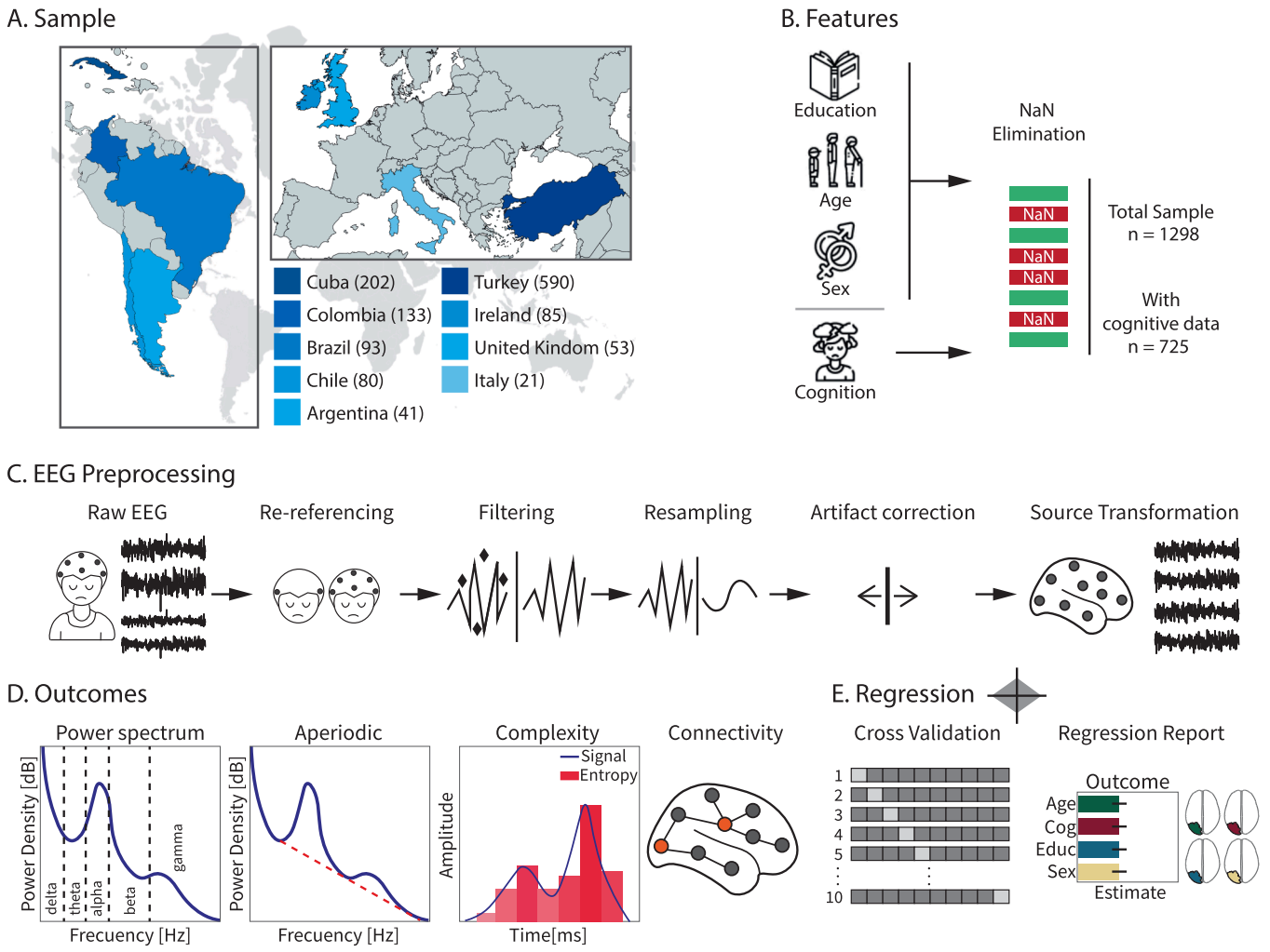


**Fig. 1. Study design. (A) Sample:** Participants were recruited from a multicenter study encompassing regions in the global south (Argentina, Brazil, Chile, Colombia, Cuba), and the global north (Italy, Ireland, Turkey, United Kingdom). **(B) Predictors:** The dataset comprised a total of 1298 participants, with cognitive data available for 725 individuals. Regression models tuned with cross validation and data partition were developed using years of education, age, sex, and cognitive state as predictors. **(C) EEG data preprocessing:** The preprocessing steps included electrode re-referencing, noise removal through signal filtering, resampling to 512 Hz, artifact removal (e.g., blinks and eye movements), and transformation into a common source space using the Automated Anatomical Labeling (AAL) atlas. **(D) Outcomes:** EEG data in the source space was used to compute four groups of metrics, categorized into power spectrum, aperiodic, complexity, and connectivity metrics. **(E) Data analysis:** Linear regressions were applied, utilizing data partitioning with an 80% training sample and a 20% testing set, cross-validated ($k = 10$ repetitions). We reported the importance of predictors and the results on the influence of each predictor on specific brain regions.

general cognitive state of 725 participants were available. The study protocol was approved by the Institutional Ethics Committee at each participating center, and all participants provided written informed consent in accordance with the Declaration of Helsinki. The data and analysis codes are freely available at the following GitHub link https://github.com/euroladbrainlat/Brain-health-in-diverse-setting. The data in the repository has been anonymized and pre-processed.

We used the G*Power 3.1.9.7 software (Faul et al., 2007) for power analysis, specifically employing an F-test for multiple linear regressions. Our study's sample size, comprising 725 subjects with cognitive measurements, surpassed the required minimum for conducting multiple linear regressions with four variables. This allows for the detection of small effect sizes (0.02 (Cohen, 1988)) with a statistical power of 0.88. Additionally, the larger total sample of 1298 subjects was adequate for performing multiple linear regressions with three variables, effectively identifying small effect sizes with a statistical power of 0.99.

### 2.2. Demographic and cognitive variables

#### 2.2.1. Demographics

The demographic information includes age at the time of assessment (in years), sex (male or female), and years of formal education. Data on gender identity was not available.

#### 2.2.2. Cognition

The general cognitive state was evaluated using the raw total score from the Mini-Mental State Examination (MMSE) (Folstein et al., 1975). This test is a widely recognized screening tool for cognitive impairment and assessing general cognitive functioning. It evaluates various cognitive domains, including orientation to time and place, short-term memory recall, working memory, language abilities, visuoconstructional skills, and basic motor commands. This instrument consists of 30 items, and each correct answer adds one point to the total score, which ranges from 0 to 30. A score of 24 or more indicates normal cognitive functioning (Creavin et al., 2016; Mukaetova-Ladinska et al., 2022; Cebi et al., 2020; Foderaro et al., 2022; Kochhann et al., 2010).

**Table 1**
Demographic and cognitive state information.

| Country | Sex | | Age | | Education | | Cognition | | |
|---|---|---|---|---|---|---|---|---|---|
| | Sex | n | Mean | SD | Mean | SD | n | Mean | SD |
| Argentina | Female | 29 | 66.76 | 8.53 | 17.03 | 2.03 | 28 | 29.04 | 0.69 |
| | Male | 12 | 66.33 | 7.92 | 15.42 | 2.94 | 12 | 28.17 | 1.85 |
| Chile | Female | 59 | 57.03 | 17.10 | 15.49 | 3.73 | 49 | 28.80 | 1.47 |
| | Male | 21 | 62.62 | 18.45 | 14.33 | 4.35 | 14 | 28.30 | 2.27 |
| Brazil | Female | 58 | 59.33 | 16.88 | 11.88 | 3.68 | 58 | 28.03 | 1.61 |
| | Male | 35 | 62.69 | 15.91 | 13.51 | 2.34 | 35 | 28.29 | 1.51 |
| Colombia | Female | 96 | 49.61 | 13.85 | 12.43 | 4.64 | 96 | 27.82 | 3.03 |
| | Male | 37 | 45.49 | 15.49 | 12.68 | 4.59 | 37 | 28.00 | 3.13 |
| Cuba | Female | 53 | 37.51 | 11.34 | 13.25 | 2.79 | 31 | 29.68 | 0.70 |
| | Male | 149 | 29.68 | 7366 | 12.99 | 2.81 | 94 | 29.28 | 1.42 |
| Italy | Female | 12 | 60.55 | 7.35 | 15.25 | 4.85 | – | — | — |
| | Male | 9 | 62.90 | 9.24 | 15.44 | 5.46 | – | — | — |
| United Kingdom | Female | 34 | 56.82 | 17.40 | 15.00 | 3.67 | – | — | — |
| | Male | 19 | 53.89 | 21.13 | 15.11 | 10.27 | – | — | — |
| Ireland | Female | 41 | 65.76 | 4.54 | 15.50 | 3.78 | 40 | 29.25 | 0.90 |
| | Male | 44 | 69.41 | 5.85 | 15.01 | 4.17 | 44 | 28.75 | 1.10 |
| Turkey | Female | 319 | 43.48 | 22.02 | 13.37 | 4.98 | 118 | 28.85 | 1.10 |
| | Male | 271 | 39.53 | 22.03 | 14.19 | 4.12 | 69 | 29.10 | 1.36 |

### 2.3. EEG data acquisition, processing, and harmonization

The EEG acquisition parameters at each center are detailed in Supplementary Table 1. Participants were situated in comfortable chairs within dimly lit, electromagnetically quiet rooms, and were advised to stay still and alert. Resting-state EEG (rsEEG) with closed eyes was recorded using various systems, encompassing distinct sensor types, calibrations, and electrode configurations (Supplementary Table 1). In some instances, EEGs with open eyes were also captured. Due to differing recording durations across centers, EEG analyses were limited to the first five minutes of each recording.

The EEG data was processed offline using a customized, automated, and validated pipeline that incorporated harmonization protocols specifically designed to mitigate batch effects and methodological variations in multi-center EEG studies (Ballesteros et al., 2023; Prado et al., 2023). The processing workflow involved several steps, including data preprocessing, EEG rescaling, spatial normalizations, and EEG source localization.

#### 2.3.1. Pre-processing

Raw EEG data was filtered between 0.5 and 40 Hz using an 8th order zero-phase shift Butterworth filter. Data were re-sampled to 512 Hz and referenced using the reference electrode standardization technique (REST) (Hu et al., 2018). Blinking, ocular artifacts and myogenic activity were corrected using two distinct ICA techniques (Delorme and Makeig, 2004): ICLabel (a tool for the classification of EEG independent components into signals and different categories of noise) (Pion-Tonachini et al., 2019) and EyeCatch (a tool for identifying eye-related ICA scalp maps) (Bigdely-Shamlo et al., 2013). ICA techniques [Infomax ICA (Górecka and Walerjan, 2011)] were exclusively used to remove ocular artifacts (blinking and eye movements). These artifacts typically fall among the first components of ICA. After ensuring artifact correction through ICA techniques (specifically, ICLabel and EyeCatch), we conducted a visual inspection of the EEG. Malfunctioning channels were replaced using weighted spherical interpolations (Kothe and Makeig, 2013).

#### 2.3.2. Normalization

The normalization process adhered to multicentric studies guidelines (Prado et al., 2022). To minimize variability across centers, Z-score transformations of EEG time series were implemented (Ballesteros et al., 2023; Prado et al., 2023a, 2023b). The normalization consisted of computing the mean voltage of each EEG channel and Z-transforming the corresponding voltage samples, considering the mean and the standard deviation of the distribution. This normalization reduces the electrode-by-electrode variability and was conducted independently for each recruitment center, therefore reducing the inter-site variability. Furthermore, a spatial normalization of EEG was performed by combining different electrode configurations, creating virtual electrodes calculated from topographic interpolation transforms. This method has been effectively utilized in studies investigating the variance between acquisition systems in contrast to between-subject and between-session variances (Melnik et al., 2017). The technique projects electrode positions onto a mesh-head model consisting of 1082 points and interpolates EEG activity. We adjusted the EEGLAB headplot (Prado et al., 2023) function to map the original EEG onto a 6067-point mesh-head model (Kothe and Makeig, 2013; Melnik et al., 2017).

#### 2.3.3. EEG source estimation

EEG source generators were estimated using the standardized low-resolution electromagnetic tomography (sLORETA) method (Pascual--Marqui, 2002). This method estimates the standardized current density at specific virtual sensors located in the cortical gray matter and the hippocampus of an average brain (MNI 305, Brain Imaging Centre, Montreal Neurologic Institute). This estimation is based on a linear, weighted summation of a unique scalp voltage configuration or the EEG cross-spectrum at the sensor level. Essentially, sLORETA serves as a distributed EEG inverse solution technique that extends from a standardized version of minimum norm current density estimation. It effectively addresses challenges associated with estimating deep sources of EEG activity and ensures precise localization, even in cases with significant correlation among nearby generators (Asadzadeh et al., 2020).

Electrode layouts were aligned with the MNI152 scalp coordinates (Mazziotta et al., 2001). When computing the sLORETA transformation matrix, a signal-to-noise ratio of 1 was selected as the regularization method. Standardized current density maps were produced using a three concentric spheres head model, in a predefined source space of 6242 voxels (with a voxel size of $5 \times 5 \times 5$ mm) of the MNI average brain. The brain was segmented into 82 brain regions using the Automated Anatomical Labeling (AAL) atlas (Rolls et al., 2015). Standarized current densities were estimated for each of the 153,600 Vage distributions comprising the five-minutes of rsEEG (sampled at 512 Hz). Standarized current density time series estimated in voxels belonging to the same AAL regions were averaged, leading to a mean time series for each brain area (Prado et al., 2023; Cruzat et al., 2023; Herzog et al., 2022).

### 2.4. EEG descriptors

We computed four categories of EEG descriptors: (i) power spectrum and (ii) aperiodic spectral metrics, (iii) complexity, and (iv) graph-theoretic measures. These categories reflect neural activity (i.e., power spectrum or aperiodic spectral metrics) (Cesnaite et al., 2023; Donoghue et al., 2020), and brain dynamics and interactions (i.e., complexity, and graph-theoretic measures) (Zappasodi et al., 2015; Vecchio et al., 2022). Power spectrum metrics are relevant in EEG data analysis, offering insights into brain activity by characterizing how signal power is distributed across various frequencies (Wang et al., 2015). These metrics establish a baseline for typical spectral activity, serving as a valuable benchmark for identifying pathological conditions (Buzsáki, 2006) The aperiodic spectral components of EEG represent non-rhythmic brain activity. These components facilitate physiological interpretations related to aging and cognition (Donoghue et al., 2020). For example, these aperiodic metrics has been linked to excitation/inhibition balance (Medel et al., 2023; Martinez-Canada et al., 2023), and electrophysiological noise (Voytek et al., 2015). Complexity metrics enable the evaluation of dynamical brain complexity, which have been explored as potential biomarkers for diagnosing mental health disorders (Tononi et al., 1994; Lau et al., 2022). Lastly, graph- theoretic metrics shed light on the structure of functional connectivity patterns and network organization (Bullmore and Sporns, 2009).

#### 2.4.1. Power spectrum metrics

Power spectrum analyses were conducted in both the canonical EEG frequency bands and the subject-specific EEG frequency bands (Babiloni et al., 2020). Canonical bands provide standardized ranges ensuring consistency and comparability across studies. However, these bands may not effectively capture individual differences (Doppelmayr et al., 1998; Bazanova and Vernon, 2014). Subject-specific bands enhance the sensitivity to detect specific physiological, cognitive, or behavioral states that might be masked when using generic bands (Klimesch, 1999). For instance, the individual alpha frequency peak (IAF) increases during childhood and slows in middle and older age (Turner et al., 2023), decreases with neurodegeneration (Moretti et al., 2004), and increases with cognitive demands (Haegens et al., 2014). Analyzing power with canonical and subject-specific frequency bands allows for a comprehensive assessment of EEG data.

The canonical frequency bands were defined as follows: delta ($\delta$): 1.5–6 Hz; theta ($\theta$): 6.5–8.0 Hz; alpha1 ($\alpha$1): 8.5–10 Hz; alpha2 ($\alpha$2): 10.5–12.0 Hz; beta1 ($\beta$1): 12.5–18.0 Hz; beta2 ($\beta$2): 18.5–21.0 Hz; beta3 ($\beta$3): 21.5–30.0 Hz; gamma ($\gamma$): 30.0–40.0 Hz. This EEG band definition is used for spectral analysis in the EEG source space with LORETA-KEY software (Grech et al., 2008). It has implemented in many studies for conducting EEG frequency-specific analyses in dementia (e.g., (Prado et al., 2023; Aoki et al., 2019)), and other conditions. (e.g. (Lee et al., 2019; Aoki et al., 2015; Aoki et al., 2019; Ouyang et al., 2020; Krause et al., 2015)).

Subject-specific frequency bands were determined using the IAF, defined as the frequency with maximum power in the alpha-frequency band, and the theta/alpha-frequency transition (TF), defined as the frequency with minimum power in the second half of theta frequency range (Martinez-Canada et al., 2023; Babiloni et al., 2020; Ince et al., 2017). The subject-specific frequency bands are defined as: $\delta$ (TF-4 to TF-2), $\theta$ (TF-2 to TF), $\alpha_{\text{low}}$ (TF to IAF), and $\alpha_{\text{high}}$ (IAF to IAF+2) (Babiloni et al., 2020). The $\beta$ and $\gamma$ frequency bands corresponded to the canonical division.

We computed both the power spectral density (PSD) and the normalized PSD (nPSD) using Welch's method with 1-second Hanning windows with 50% overlap. Subsequently, we calculated the mean of the nPSD in each frequency band (equivalently percent power) (Li et al., 2007) and the percent of the nPSD of a given frequency band relative to the total nPSD (relative power density) (Wang et al., 2015; Babiloni et al., 2020).

#### 2.4.2. Aperiodic spectral metrics

We computed the aperiodic components of the EEG power spectral density (PSD): the 1/f slope ($a$), knee ($k$), and offset ($b$) (Martinez-Canada et al., 2023; Pathania et al., 2021; van Nifterick et al., 2023). We applied the fitting oscillations and one-over-F (FOOOF) algorithm to the PSD, covering the frequency band from 0.5 to 40 Hz, peak width limits from 1 to 6 Hz, maximum number of peaks of 6, minimum peak height of 0.2, and peak threshold of 2.0 (Martinez-Canada et al., 2023; Pathania et al., 2021; van Nifterick et al., 2023). The FOOOF algorithm was designed to model the aperiodic component of the PSD (Donoghue et al., 2020), using a Lorentzian function as follows:

$$A = b - \log(k + F^{x})$$

where $A$ is the aperiodic component, $b$ is the offset, $x$ is the exponent, and $x$=-$a$.

#### 2.4.3. Complexity metrics

Complexity descriptors of the EEG source space provide insights into the dynamics of different brain regions and their interactions. A high complexity value in an EEG signal indicates an increased degree of irregularity, indicating that the EEG is less predictable. This is often associated with a healthy and alert brain state (Medel et al., 2023). Conversely, a low comlexity values suggests a more regular or repetitive signal, could be observed in pathological states (Sun et al., 2020) anaesthesia or deep sleep (Sarasso et al., 2021; Boncompte et al., 2021). Fractal dimension (FD), permutation entropy (PE), Wiener Entropy (WE), and spectral structure variability (SSV) (Sun et al., 2020; Burns and Rajan, 2015) were computed to assess the complexity of EEG signals, with code sourced from a GitHub repository (https://github.com/tfburns/MATLAB-functions-for-complexity-measures-of-one-dimensional-signals) (Burns and Rajan, 2016). We include measures of predictability (FD) as well as regularity (PE, WE, SSV), which represent the two key aspects of brain dynamics (Lau et al., 2022). Predictability refers to the ability to anticipate the temporal evolution of the system's states, while regularity measures the frequency and pattern of repetitions in the system's trajectory (Lau et al., 2022). Changes in FD are linked to variations (Zappasodi et al., 2015) and cognition (Smits et al., 2016; Hemmati et al., 2013). Similarly, both PE and WE have been associated with individual differences in age (Al Zoubi et al., 2018; Shumbayawonda et al., 2018) and cognition (Parbat and Chakraborty, 2021; Seker et al., 2021). These metrics collectively capture broad conceptions of complexity (Burns and Rajan, 2015). The equations for complexity metrics are described below.

**Fractional dimension:** The FD is a statistic index of complexity details in a patter and can be expresed as:

$$FD = a(NLD - NLD_0)^{k}$$

where $a$, $k$ y $NLD_0$, was set to the suggested parameters values: 1.9079, 0.18383 y 0.097178, respectively (Kalauzi et al., 2009). The $NLD$ was calculate as:

$$NLD = \frac{1}{N}\sum_{i=2}^{N} |y_n(i) - y_n(i-1)|$$

where $y_n(i)$ represents the *ith* signal sample after amplitude normalization.

**Permutation entropy:** The PE is an ordinal-based non-parametric metric of the temporal dependence structure in linear or non-linear time series. Therefore, PE can be expressed as follows:

Considering a time series represented by $x_t$, con $t = 1, \ldots, T$, and the embedded vector $X_t = [X_t + X_{t+l}, \ldots, + X_{t+(n-1)}]$, where $n$ is the embedding dimension and $l$ is the lag. Then, the vector $X_t$ is arranged from smallest to largest. Finally, PE was defined as:

$$PE = -\sum_{n=1}^{n!} p(\pi)\ln(p)$$

where $p(\pi) = f(\pi)/(T-(n-1)l)$ y $f(\pi)$ represents the frequency of the symbols of length $n$ derived from the ordinal relationships between $Xt$. (Ouyang et al., 2013)

**Wiener entropy and spectral structure variation**: The WE, alternatively referred to as spectral flatness or tonality coefficient, signifies the uniform distribution of signal energy across the frequency domain. This metric provides a quantifiable measure of how closely the signal mirrors a sinusoidal function, as opposed to exhibiting characteristics reminiscent of noise. The spectral flatness measure (SFM) was used to quantify spectral structure (Singh, 2011), and the equation for its calculation is as follows:

$$SFM(t) = log\frac{\left[\prod_{i=1}^{N} S(t,f)\right]^{\frac{1}{N}}}{\left(\frac{1}{N}\right)\sum_{i=1}^{N} S(t,f)}$$

where N is the number of points in the Fourier transform, and $S(t,f)$ is the associated power at each frequency component. Finally, the Wiener entropy is calculated as the average of $SFM(t)$, and the spectral structure variability is calculated as the variance of $SFM(t)$.

### 2.4.4. Connectivity graph metrics

Calculating graph metrics required determining functional connectivity across the entire space of different brain regions. Functional connectivity was assessed in the time-domain using information theoretic measures, which were calculated with custom Matlab codes (Prado et al., 2023; Herzog et al., 2022). These measures were derived using the Gaussian copulas approximation (Ince et al., 2017), a robust computational framework that combines copulas statistical theory with an analytic solution for the entropy of multivariate Gaussian distributions. The incorporation of Gaussian copulas-based methods strengthens the robustness and cost-effectiveness of our methodology, resulting in a reduction of computational time required for functional connectivity calculations. We computed both pairwise and high-order interactions metrics, specifically mutual information (MI) (Prado et al., 2023; Herzog et al., 2022; Santamaria-Garcia et al., 2023), conditional mutual information (CMI) (Prado et al., 2023; Ince et al., 2017), and organizational information (O_info) (Prado et al., 2023) metrics (Supplementary Data S1). MI gauges the shared information between two random variables (or time series), while CMI assesses the shared information between two random variables (or time series) with respect to a specified third variable. Finally, O_info, an extension of Shannon's mutual information, enhances our understanding of the crucial characteristics of multivariate systems, especially those involving high-order interactions (Herzog et al., 2022). Information theory metrics surpass traditional measures like coherence or phase locking value because they can capture non-linear interactions (Imperatori et al., 2019; Kida et al., 2016) and provide better results(109). This is crucial for exploring brain dynamics, where complex non-linear interactions among neural regions shape patterns of functional connectivity (Imperatori et al., 2019; Kida et al., 2016).

Measures of segregation, integration, and global metrics were included to measure complementary dimensions of network topology (Bullmore and Sporns, 2009; Rubinov and Sporns, 2010). Global Efficiency provides insights into the efficiency of information exchange across the entire network, crucial for global information processing (Rubinov and Sporns, 2010). Transitivity measures the prevalence of clustered connectivity, reflecting localized, interconnected communities key for local processing and network segregation (Rubinov and Sporns, 2010). Small-worldness captures the balance between random and regular networks, indicating an optimal organization of localized and distributed processing, and integration and segregation, enhancing network efficiency and robustness (Bassett and Bullmore, 2017). Lastly, density quantifies the overall connectivity of the network, offering a direct assessment of the complexity and connectivity level (Rubinov and Sporns, 2010). All these measures have been shown to be sensitive to individual differences in age (Javaid et al., 2022; Meunier et al., 2009; Achard and Bullmore, 2007; Onoda and Yamaguchi, 2013), sex (Miraglia et al., 2015) and cognition (Finnigan and Robertson, 2011; Bullmore and Sporns, 2009; Iinuma et al., 2022; McBride et al., 2014; Liao et al., 2017) . The equations of these metrics are described below.

**Connection weight**: The connection weight expresses the strength with which nodes are linked, where $w_{ij}$ is the connection weight between node $i$ and node $j$.

**Weighted shortest path length**: The shortest path length is a fundamental metric to evaluate integration, which is defined as:

$$d_{ij} = \sum_{a_{uv} \in gi \leftrightarrow j} f(w_{uv})$$

where $f$ serves as a mapping from weight to length, and $gi \leftrightarrow j$ represents the shortest weighted path between $i$ and $j$.

**Weighted characteristic path length**: The characteristic path length is a measure employed to evaluate communication efficiency in a weighted network. The equation for its calculation is as follows:

$$L = \frac{1}{n}\sum_{i}\frac{\sum_{j\neq i} d_{ij}}{n-1}$$

where $n$ represents the number of nodes in the network, and $d_{ij}$ is the length of the shortest path between node $i$ and node $j$.

**Number of triangles**: The number of triangles is a fundamental metric to evaluate segregation, which is defined as:

$$t_i = \frac{1}{2}\sum_{j,h}\left(w_{ij}w_{ih}w_{jh}\right)^{\frac{1}{3}}$$

where $t_i$ is the weighted geometric mean of triangles around $i$, $j$ and $h$ are indices representing the neighboring nodes of $i$ in the weighted matrix.

**Weighted degree**: The weighted degree is a measure employed to evaluate the importance or connectivity of a node in a weighted network. This metric can be calculated as follows:

$$k_i = \sum_{j} w_{ij}$$

where $k_i$ is the degree of a node $i$.

**Weighted clustering coefficient**: The clustering coefficient is a metric used to evaluate the tendency of nodes in a network to form local groupings or clusters. The equation is as follows

$$C = \frac{1}{n}\sum_{i}\frac{2t_i}{k_i(k_i-1)}$$

where $t_i$ is the number of triangles around $i$ and $k_i$ is the weighted degree of a node $i$.

**Weighted global efficiency**: Global efficiency was employed to assess integration, crucial in quantifying the effective sharing of information across the brain, essential for coordinated cognitive activity. This metric evaluates the network's ability to exchange information globally (Yu et al., 2021; Stanley et al., 2015). The equation for its calculation is as follows.

$$E = \frac{1}{n(n-1)}\sum_{i\neq j}\frac{1}{d_{ij}}$$

where $n$ represents the number of nodes in the network, and $d_{ij}$ is the length of the shortest path between node $i$ and node $j$.

**Weighted transitivity**: Transitivity was selected to measure segregation due to its reflection of local interconnectivity, indicating the

tendency of nodes to form closed clusters or triads. It serves as an indicator of local connectivity (Rubinov and Sporns, 2010) and can be expressed as follow.

$$T = \frac{\sum_i 2t_i}{\sum_i k_i(k_i - 1)}$$

where $t_i$ is the number of triangles around $i$ and $k_i$ is the weighted degree of a node $i$.

**Weighted density**: Density served as global measure, indicating the overall connectedness of the network addressing complexity and resilience of brain functioning (Rubinov and Sporns, 2010). The equation for its calculation is as follows.

$$D = \frac{\sum_{i \neq j} w_{ij}}{n(n-1)}$$

where $w_{ij}$ represents the weight of the connection between node i and node j, and n is the total number of nodes in the network.

**Weighted small-worldness**: Small-worldness was utilized to evaluate both integration and segregation, capturing the optimal balance between specialized processing within clusters and the global integration essential for comprehensive brain functionality. A network exhibits small-world characteristics if it displays a high clustering coefficient (reflecting segregation) and a short characteristic path length (indicating integration) (Rubinov and Sporns, 2010; Bassett and Bullmore, 2017; Yu et al., 2021).

The commonly used measure to quantify small-worldness in a network includes the clustering coefficient (C) and the characteristic path length (L). The formula for small-worldness is expressed as the ratio of the observed clustering coefficient in the network (C) to the expected clustering coefficient in a random graph with the same number of nodes and edges ($C_r$), normalized by the observed characteristic path length in the network (L) and the expected characteristic path length in the random graph ($L_r$).

$$\sigma = \frac{C/C_r}{L/L_r}$$

A crucial difference between transitivity and the clustering coefficient is found in the normalization procedure. Clustering is normalized individually for each node, while transitivity is normalized across the entire node set (Rubinov and Sporns, 2010).

### 2.5. Simplification of the EEG analytical domain

To streamline the analysis of spectral and complexity results from EEG data, we adopted two complementary approaches. Initially, anatomically and functionally related AAL regions were merged to form more consolidated regions of interest (ROIs), as detailed in Supplementary Table 3. Subsequently, we refined the EEG analytical space by applying specific statistical criteria. The methodology for these processes is elaborated in the subsequent sections.

#### 2.5.1. Region selection for analysis

We combined regions from the AAL atlas to generate ten cohesive ROIs. This approach involved two critical criteria: (i) grouping together brain regions associated with a specific cortical gyrus (e.g., superior, middle, and inferior orbital gyri) into a single ROI, and (ii) assembling neighboring regions with established functional coupling, such as the Rolandic operculum and insula. The proposed method restructures EEG analysis by concentrating on ROIs that include both structurally and functionally related regions, rather than analyzing each small region in isolation. We utilized a mean averaging approach, calculating the average value of the metrics derived from the signals of the regions within the AAL atlas that are associated with each ROI. This simplification enhances data interpretation and facilitates the identification of patterns or significant features in brain activity.

#### 2.5.2. Statistical reduction of spectral and complexity features

To refine the analysis of spectral and complexity metrics, we applied statistical criteria. Specifically, ROIs demonstrating statistically significant relative power density and equivalent percent power (Wang et al., 2015; Jeong et al., 2021; Moretti et al., 2004) were identified through mean-vs-zero non-parametric permutation tests ($\alpha = 0.05$; 5000 randomizations (Manly, 1997)). This refinement, applied to both canonical and individual EEG band classifications (Babiloni et al., 2020), was carried out for each frequency band. The results were then adjusted for multiple comparisons using the Benjamini and Hochberg False Discovery Rate (FDR) method. ROIs representing the Individual Alpha Frequency (IAF) (Klimesch, 1999; Moretti et al., 2004) were those displaying statistically significant α activities. Similarly, ROIs indicative of the θ-α transition (TF) (Klimesch, 1999; Moretti et al., 2004) were those with statistically significant θ activity. Moreover, the analytical space of aperiodic (Martinez-Canada et al., 2023; Pathania et al., 2021; van Nifterick et al., 2023) and complexity (Sun et al., 2020; Burns and Rajan, 2015) metrics was further reduced by employing mean-vs-zero non-parametric permutation tests, followed by correction using the Benjamini and Hochberg FDR method.

### 2.6. Multiple linear regression models

We used multiple linear regression models to understand the relationship between predictors and outcome variables (Bishop, 2006). The regression models were constructed using the four predictors outlined in Section 2.2. We constructed an individual regression model for each ROI. Regression models were generated and categorized based on the highest-rated predictors. This approach allowed us to separate the results into three distinct groups according to the top-rated predictor. The first group prioritized age as the top-rated predictor, the second emphasized education, and the third focused on cognition. None of the models identified gender as the most important predictor. The mathematical representation of the linear regression model is:

$$Y = B_0 + B_1 x + B_1 x_1 + B_2 x_2 + B_n x_n + \epsilon$$

where $Y$ is the outcome variable, $B_0$ is the intercept, $B = [B_1,\ B_2,\ \ldots,\ B_n]$ is the coefficients vector of the independent variables matrix $X = [x_1,\ x_2,\ \ldots,\ x_n]$ and $\epsilon$ represents the error term. The coefficients $B_1,\ B_2,\ \ldots,\ B_n$ are determined using the least squares method, which aims to minimize the sum of the squared differences (errors) between the observed values (actual values) and the values predicted by the model. The formulas to calculate the coefficients are:

$$B = \left(X^T X\right)^{-1} X^T Y$$

where $X^T$ is the transpose of matrix of vector X .

The EEG parameters obtained from the chosen ROIs (see Supplementary Table 3) and the connectivity outcomes estimated in whole-brain analyses were utilized as inputs for the multiple linear regression models described above.

### 2.7. Data partition

Models were trained on a training sample (80%) and tested in a testing set (20%), with $k = 10$ folds (Muller and Guido, 2018). For each iteration, we computed the estimation coefficients for the predictors, R-squared, Cohen's $f^2$, Fisher's F of the model, and the model's significance. We reported the mean estimation values for each predictor along with their standard deviation, average R-squared and Cohen's $f^2$ (Selya et al., 2012), and overall Fisher's F. To determine the overall model significance, we combined the model's p-values obtained in each iteration using the Fisher method (Fisher, 1992).

### 2.8. Statistical criteria for the reduction of feature space for frequency and complexity metrics

A further reduction of the analytical space was conducted using statistical criteria. To this end, ROIs with statistically significant relative power density and equivalent percent power (Wang et al., 2015; Moretti et al., 2004; Jeong et al., 2021) were selected by implementing mean-vs-zero non-parametric permutation tests ($\alpha = 0.05$; 5000 randomizations (Manly, 1997)). This analysis was conducted for each frequency band, using both canonical and individual (Babiloni et al., 2020) EEG band classifications. Results were corrected for multiple comparisons using the Benjamini and Hochberg FDR method (Benjamini and Hochberg, 1995). Representative ROIs for IAF (Klimesch, 1999; Moretti et al., 2004) were those for which θ and α activities were statistically significant. Likewise, ROIs for TF (Klimesch, 1999; Moretti et al., 2004) were those for which θ activity was statistically significant. Furthermore, mean-vs-zero non-parametric permutation tests followed by Benjamini and Hochberg FDR was the method selected for further reducing the analytical space of the aperiodic (Martinez-Canada et al., 2023; Pathania et al., 2021; van Nifterick et al., 2023) and complexity (Sun et al., 2020; Burns and Rajan, 2015) metrics.

### 2.9. Quality of the signal

We conducted additional analyses to confirm that the number of electrodes does not impact signal quality and does not interfere with the observed effects. We calculated the Overall Data Quality (OQD) index in the source space, using the methodology proposed by Zhao et al. (2023), and conducted a linear regression to verify that the number of channels cannot predict signal quality. We used the number of channels as a predictor and the quality of the final signals as the outcome. The method for calculating OQD segmented into 1-second epochs, each labeled as 1 for low-quality epochs or 0 for high-quality epochs. The OQD represents the percentage of EEG epochs with good quality, ranging from 0 for signals where all epochs were classified as low quality, to 100 for signals where all epochs were classified as high quality (Zhao et al., 2023).

## 3. Results

For each type of EEG descriptor (spectral, complexity, and connectivity EEG outcomes), we categorized the regression models based on their top-rated predictors, resulting in three distinct groups according to the best-evaluated predictor. The first group prioritized age as the best-evaluated predictor, the second group emphasized education, and the third group centered on cognition. None of the models identified sex as the most important predictor. For each group of models and sets of EEG outcomes, we reported the three models with the highest $R^2$ values. Additionally, we reported the adjusted $R^2$. In the Supplementary Material (Supplementary Figures 1–3), we provided an assessment of the model fit quality using Q-Q plots and residual vs. fitted values plots. In most cases, the results for the total sample and the subsample with available cognitive data were similar; therefore, we report the results for the latter. Further details on the results for the total sample are provided in Supplementary Tables 1 to 7.

Some participants had portions of the recording with their eyes open (Supplementary Table 1). Therefore, we analyzed data only from participants who underwent eye-close rsEEG exclusively. These results were comparable to those reported with the entire sample, and are detailed in Supplementary Tables 8 - 11. In addition, we checked for collinearity among the predictors (see Supplementary S2 and Supplementary Figure 4) and conducted supplementary analyses using Ridge regressions (Supplementary Tables 12–15), which is a suitable method for predictors exhibiting collinearity (Tsigler and Bartlett, 2024). The results obtained with Ridge were comparable to the previous results.

We conducted additional analyses to ensure that variations in the number of channels across recruitment centers did not influence the results. We applied a linear regression to check if the number of channels predicts signal quality in the source space. The results showed that the model was not significant (Supplementary Table 16). Finally, we conducted an analysis of the correlation across the outcomes reported in the main results (see Supplementary S3, Supplementary Figure 5, and Supplementary Tables 17–20) to assess the effect of their correlation on the reported effects.

### 3.1. Age, education and cognition as the best predictors of power spectrum metrics

Statistical descriptors for all the regression models reported here are shown in Table 2.

The two regression models predicting age with the highest $R^2$ values had subject-specific $\alpha_{low}$ equivalent power as the EEG outcome measure. The third one had cannonical γ equivalent power. The first model reached the highest values in the left occipital region, the second in the left parietal region, and the third in the left orbitofrontal region (Table 2A and Fig. 2A). For all three models, the most important and significant predictors were age and cognition. In the model for the left occipital region, sex was the third most important predictor. For the other two models, education was the third significant predictor. When analyzing the total sample, the results for the three models remained significant, although $R^2$ values decreased (Fig. 2A, and Supplementary Table 4A).

For education as the best rated predictor, the three models with the highest $R^2$ values had IAF as the outcome measure. The model with best scores corresponded with the right medial frontal gyrus, and revealed education, cognition, age, and sex as significant predictors (Fig. 2B and Table 2B). In the second and third models, the highest values were reached in the left orbitofrontal cortex and the left inferior frontal gyrus, respectively, education and age were the significant predictors displaying similar values. Sex and cognition were significant in the best model, but not in the other two. In the total sample, $R^2$ values were low, but the models remained statistically significant (Fig. 2B and Supplementary Table 4B).

When cognition was the best-evaluted predictor, the two best models estimated canon $\alpha_2$ relative power metrics more accurately. The third one performed better in estimating subject-specific αlow equivalent power. The first two models were in the left occipital regions and the third one in the right parietal region (Fig. 2C and Table 2C). For the three models, cognition and age emerged as the most important and significant predictors. Sex reached significance in the three models, but with lower estimates. Education was not statistically significant in any model. In the total sample, the models were also statistically significant, but showing a decrease in the $R^2$ values (Fig. 2C and Supplementary Table 4C).

### 3.2. Age and cognition as the best predictors of aperiodic spectral metrics

Statistical values for all models reported here are shown in Table 3.

For age as the top predictor, the three best-evaluated models had slope as the outcome metric. These models were placed in the left temporal region, the right temporal region, and the left hippocampus, respectively (Fig. 3A and Table 3A). In all three models, age and cognition emerged as the most important and significant predictors. In the first model, sex also reached significance, but not in the second and the third one. Education was not statistically significant in any model. In the total sample, the models were also statistically significant, but with lower $R^2$ values (see Fig. 3A and Supplementary Table 5A).

The best model with cognition as the best-evaluated predictor, estimated slope metrics more accurately. The second and the third models performed better in estimating offset metrics. The best model of cognition was in the left occipital region, the second in the left temporal region and the third in the left hippocampus (Fig. 3C and Table 3B). It is worth noting that, although reaching significance, all these models

**Table 2**
Results for the power spectrum metrics on the subsample with available cognitive data.

A. Models with age as the best evaluated feature

Left occipital region (subj spec $\alpha_{low}$ equivalent power), $F = 129.36$, $p < 1e\text{-}15$, $R^2 = 0.27$, $R^2$ adjusted = 0.26, CI =0.07, $F^2$ =0.36

| Predictors | Estimate | t value | p value |
|---|---|---|---|
| Age | −0.01592 | 6.563429 | <1e-15 |
| Cognition | 0.009309 | 2.016705 | 5.81E-08 |
| Sex | −0.00224 | 1.878269 | 6.25E-07 |
| Education | −0.00181 | 0.470018 | 0.917864 |

Left parietal region (subj spec $\alpha_{low}$ equivalent power), $F = 125.99$, $p < 1e15$, $R^2 = 0.26$, $R^2$ adjusted = 0.26, CI = 0.047, $F^2 = 0.35$

| Predictors | Estimate | t value | p value |
|---|---|---|---|
| Age | −0.01568 | 6.421747 | <1e-15 |
| Cognition | 0.008753 | 1.8797 | 7.22E-07 |
| Education | −0.00388 | 1.005555 | 0.074094 |
| Sex | −0.00264 | 2.201016 | 1.19E-09 |

Left orbitofrontal region (canonical γ equivalent power), $F = 120.68$, $p < 1e15$, $R^2 = 0.25$, $R^2$ adjusted = 0.25, CI = 0.05, $F^2 = 0.34$

| Predictors | Estimate | t value | p value |
|---|---|---|---|
| Age | 0.014329 | 7.140123 | <1e-15 |
| Cognition | 0.008861 | 2.333015 | 8.69E-11 |
| Education | −0.00572 | 1.790197 | 2.97E-06 |
| Sex | 0.000972 | 0.990132 | 0.07891 |

B. Models with education as the best evaluated feature

Right medial frontal gyrus (IAF), $F = 18.19$, $p < 1e15$, $R^2 = 0.05$, $R^2$ adjusted = 0.05, CI = 0.025, $F^2 = 0.04$

| Predictors | Estimate | t value | p value |
|---|---|---|---|
| Education | −1.01733 | 1.670948 | 2.23E-05 |
| Cognition | 0.944278 | 1.283513 | 0.004605 |
| Age | −0.79489 | 2.075072 | 1.58E-08 |
| Sex | −0.25695 | 1.36426 | 0.001602 |

Left inferior frontal gyrus (IAF), $F = 12.22$, $p < 1e15$, $R^2 = 0.03$, $R^2$ adjusted = 0.03, CI = 0.04, $F^2 = 0.024$

| Predictors | Estimate | t value | p value |
|---|---|---|---|
| Education | −0.96513 | 1.353999 | 0.001883 |
| Age | −0.89932 | 2.00498 | 6.22E-08 |
| Cognition | 0.265095 | 0.330327 | 0.990641 |
| Sex | −0.19967 | 0.906448 | 0.149072 |

Left orbitofrontal region (IAF), $F = 9.59$, $p < 1e15$, $R^2 = 0.026$, $R^2$ adjusted = 0.02, CI = 0.07, $F^2 = 0.01$

| Predictors | Estimate | t value | p value |
|---|---|---|---|
| Education | −0.99361 | 1.475303 | 0.000392 |
| Age | −0.96511 | 2.275339 | 2.48E-10 |
| Cognition | 0.266543 | 0.315654 | 0.996028 |
| Sex | −0.15246 | 0.732682 | 0.415125 |

C. Models with cognition as the best evaluated feature

Left occipital region (canonical $\alpha_2$ relative power), $F = 69.25$, $p < 1e15$, $R^2 = 0.16$, $R^2$ adjusted = 0.16, CI = 0.06, $F^2 = 0.18$

| Predictors | Estimate | t value | p value |
|---|---|---|---|
| Cognition | 0.000834 | 2.464738 | 3.98E-12 |
| Age | −0.00071 | 4.037384 | <1e-15 |
| Education | −0.0002 | 0.718862 | 0.436808 |
| Sex | −0.00011 | 1.299236 | 0.003882 |

Left occipital region (canon $\alpha_2$ equivalent power), $F = 69.25$, $p < 1e15$, $R^2 = 0.16$, $R^2$ adjusted = 0.16, CI = 0.06, $F^2 = 0.18$

| Predictors | Estimate | t value | p value |
|---|---|---|---|
| Cognition | 0.005837 | 2.464738 | 3.98E-12 |
| Age | −0.00497 | 4.037384 | <1e-15 |
| Education | −0.00141 | 0.718862 | 0.436808 |
| Sex | −0.00078 | 1.299236 | 0.003882 |

Right occipital region (subject spec $\alpha_{high}$ equivalent power), $F = 68.55$, $p < 1e15$, $R^2 = 0.16$, $R^2$ adjusted = 0.16, CI = 0.09, $F^2 = 0.19$

| Predictors | Estimate | t value | p value |
|---|---|---|---|
| Cognition | 0.007048 | 2.334146 | 9.2E-11 |
| Age | −0.00704 | 4.415218 | <1e-15 |
| Sex | −0.00134 | 1.698314 | 1.38E-05 |
| Education | −0.00082 | 0.347323 | 0.979016 |

showed $R^2$ values lower than 0.1. In the three models, cognition and age were the most important and significant predictors. Sex and education did not reach significance in any model. In the total sample, the models were also statistically significant, but with lower $R^2$ values (Fig. 3C and Supplementary Table 5B).

The models in which education was the best-rated predictor were not statistically significant (Fig. 3B).

### 3.3. Cognition as the best predictor of complexity metrics

Statistical values for all models reported here are shown in Table 4. There were no models where age, education or sex were identified as the most highly valued predictors.

For cognition as the top predictor, the FD and the WE metrics in the whole brain were the main outcomes in the two best models. The third model performed better in spectral structure variation. In all the models, cognition showed much higher estimates compared to other predictors. For the best two models, age, and sex were also significant predictors. In the third model, sex was significant. Education did not reach significance in any model (Table 4A and Fig. 4C). In the total sample, the models were also statistically significant but with an important decrease in $R^2$ values (Fig. 3C and Supplementary Table 6A).

### 3.4. Age and education as the best predictors of graph-theoretic measures

Statistical values for all models reported here are shown in Table 5.

When age was the top predictor, the best model estimated transitivity in the CMI matrix more accurately. The second and the third ones performed better in estimating global efficiency and small-worldness in the MI and CMI matrices, respectively. For all the three models, age and education were the most important and significant predictors. In the first model, cognition was also significant. Sex did not reach significance in any model (Fig. 4A and Table 5A). In the total sample, the models were also statistically significant with almost the same performance as in the subsample (Fig. 4A and Supplementary Table 7A).

For education as the top predictor, the best model had transitivity as outcome, the second one global efficiency and the third one small-worldness, all of them in the organizational information. The three models revealed education and age as the most important and significant predictors. Cognition and sex were not statistically significant in any model (Table 5B and Fig. 4B). The models were also statistically significant in the total sample (Fig. 4B and Supplementary Table 7B).

There were no models where cognition was identified as the most highly valued predictor.

## 4. Discussion

This study aimed to characterize EEG-derived endophenotypes based on demographic and cognitive factors across a diverse sample of participants. Despite multimodal diversity and heterogeneity (diverse populations, data acquisition, multicentric assessments, amplifiers, number and type of electrodes), individual differences shaped electrophysiological brain dynamics. Age emerged as the most robust and systematic predictor of EEG signals, followed by cognition. Education and sex were less influential predictors. Power spectrum activity and graph-theoretic measures were the most sensitive in capturing individual differences. Results are relevant for better understanding the individual differences that lead to diversity. The use of more affordable and scalable measures, such as EEG metrics, could be instrumental in creating future brain charts. The present findings may challenge traditional interpretations of case-control differences in brain signatures, emphasizing the influence of demographic and cognitive factors in brain-phenotype associations.

Age was associated with changes power spectrum and aperiodic spectral activity and less integrated and segregated networks. Age predicted a decrease in alpha power at parieto-occipital regions (Trondle et al., 2023; Donoghue et al., 2020), while the opposite direction was observed for gamma power in orbitofrontal regions (Rempe et al., 2023; Hunt et al., 2019). This pattern of results could be explained by the gradual loss of cholinergic function in the basal forebrain with age

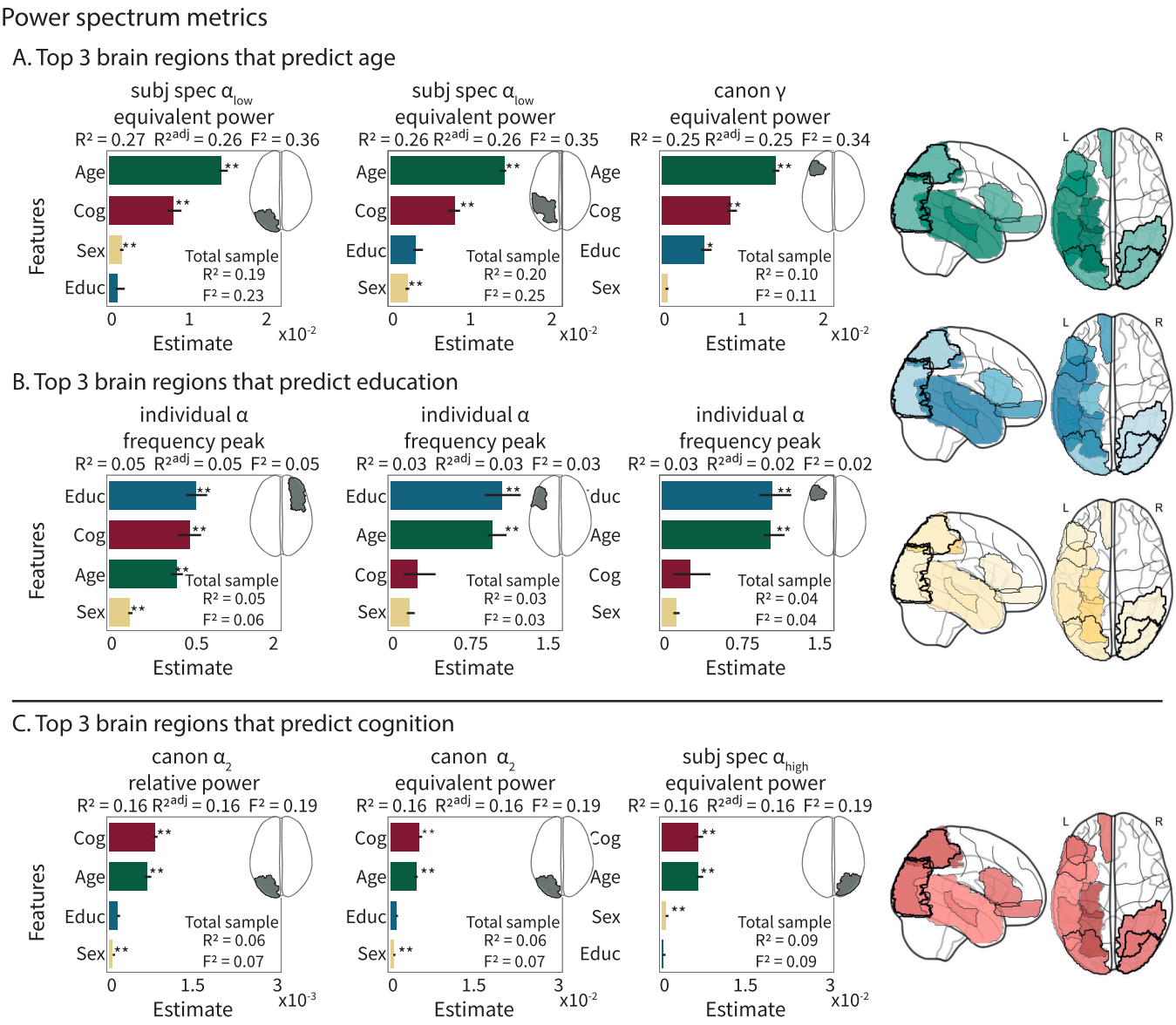


**Fig. 2. Power spectrum metrics results. (A)** The three best models, where age was the best-evaluated feature, estimated low-frequency metrics more accurately. Age and cognition emerged as the most significant predictors with the highest evaluation. While sex was statistically significant, its impact in the models was minimal. When analyzing the total sample, $R^2$ values decreased, but the predictors remained significant. **(B)** The three best models, where education was the best-evaluated feature, exhibited low $R^2$ values but maintained statistical significance. These models IAF metrics more accurately. Both education and age demonstrated significance and displayed similar values in the models. Sex and cognition were significant in the best model. In the total sample, $R^2$ was very low, but the models remained statistically significant. **(C)** The three best models, where cognition was the best-evaluated feature, had a similar structure to panel A, but they estimated high and canonical frequencies more accurately. Cognition was the best-evaluated feature, but age reached almost the same value. Education did not reach statistical significance. For the total sample, there was a significant decrease in $R^2$. The brains in the right column represent the intensity of predictors in the respective brain regions for statistically significant models, for the subsample with cognitive data. The models in occipital regions were the most significant ones, with parietal regions also demonstrating significant models. Some additional regions in the left hemisphere emerged, including the inferior, middle and orbital frontal gyri. The statistical values for the models with the complete sample are provided within each box.

(Schreckenberger et al., 2004) which is associated with diminished cholinergic input in the thalamus (Hindriks and van Putten, 2013; Pfurtscheller and Lopes da Silva, 1999), leading to decreased power in alpha oscillations (Trondle et al., 2023; Schliebs and Arendt, 2011). Conversely, increased gamma in the orbitofrontal cortex suggests a potential compensatory mechanism associated with age-related changes in frontal lobes, regions susceptible to developmental and aging processes (Rempe et al., 2023).

The decrease in the aperiodic slope with increasing age aligns with previous results (Hill et al., 2022; Merkin et al., 2023; Trondle et al., 2023) and supports the proposed association between older ages and increased asynchronous background neuronal firing (Trondle et al., 2023; Donoghue et al., 2020). As age advances, there is an increase in random and spontaneous neural activity (Cremer and Zeef, 1987) and a decrease in the signal-to-noise ratio (Voytek et al., 2015). This reduction in signal-to-noise may stem from heightened spontaneous/baseline neural spiking activity (Cremer and Zeef, 1987), disrupting neural communication fidelity and potentially contributing to typical age-related cognitive decline (Voytek et al., 2015). Furthermore, the findings of age-related decreases in alpha power and a flattened aperiodic slope are highly compatible. These two phenomena may reflect aspects of the same neurobiological changes (Trondle et al., 2023). Decreased thalamic inhibitory control over cortical areas, due to impaired cholinergic input, is reflected in diminished cortical alpha

**Table 3**
Results for aperiodic spectral metrics on the subsample with available cognitive data.

| A. Models with age as the best evaluated feature | | | |
|---|---|---|---|
| Left temporal region (slope), $F = 50.12$, $p < 1e15$, $R^2 = 0.12$, $R^2$ adjusted = 0.12, CI = 0.06, $F^2 = 0.13$ | | | |
| Predictors | **Estimate** | **t value** | **p value** |
| Age | −1.43333 | 3.930518 | <1e-15 |
| Cognition | 0.856312 | 1.208334 | 0.01079 |
| Education | −0.24692 | 0.469671 | 0.900581 |
| Sex | −0.23427 | 1.30627 | 0.003451 |
| Right temporal region (slope), $F = 41.16$, $p < 1e15$, $R^2 = 0.10$, $R^2$ adjusted = 0.10, CI = 0.06, $F^2 = 0.11$ | | | |
| Predictors | **Estimate** | **t value** | **p value** |
| Age | −1.30515 | 3.67437 | <1e-15 |
| Cognition | 0.877152 | 1.278449 | 0.005588 |
| Education | −0.18117 | 0.338246 | 0.986777 |
| Sex | −0.16609 | 0.947864 | 0.117285 |
| Left hippocampus (slope), $F = 37.40$, $p < 1e15$, $R^2 = 0.10$, $R^2$ adjusted = 0.09, CI = 0.05, $F^2 = 0.10$ | | | |
| Predictors | **Estimate** | **t value** | **p value** |
| Age | −1.27768 | 3.474221 | <1e-15 |
| Cognition | 0.896495 | 1.265951 | 0.006104 |
| Education | 0.136882 | 0.272953 | 0.999229 |
| Sex | −0.13321 | 0.732632 | 0.425399 |
| **B. Models with cognition as the best evaluated feature** | | | |
| Left occipital (slope), $F = 26.55$, $p < 1e15$, $R^2 = 0.07$, $R^2$ adjusted = 0.07, CI = 0.025, $F^2 = 0.07$ | | | |
| Predictors | **Estimate** | **t value** | **p value** |
| Cognition | 1.226913 | 1.675558 | 2.23E-05 |
| Age | −1.01193 | 2.689972 | 1.39E-14 |
| Education | −0.11348 | 0.282464 | 0.998198 |
| Sex | −0.04598 | 0.324079 | 0.991951 |
| Left Temporal (offset), $F = 22.15$, $p < 1e15$, $R^2 = 0.06$, $R^2$ adjusted = 0.06, CI = 0.03, $F^2 = 0.05$ | | | |
| Predictors | **Estimate** | **t value** | **p value** |
| Cognition | 1.931183 | 1.398192 | 0.001154 |
| Age | −1.76673 | 2.492283 | 1.74E-12 |
| Education | −0.61812 | 0.574947 | 0.792155 |
| Sex | −0.35667 | 1.023012 | 0.061897 |
| Left hippocampus (offset), $F = 18.55$, $p < 1e15$, $R^2 = 0.05$, $R^2$ adjusted = 0.05, CI = 0.03, $F^2 = 0.05$ | | | |
| Predictors | **Estimate** | **t value** | **p value** |
| Cognition | 2.300525 | 1.679279 | 2.35E-05 |
| Age | −1.58893 | 2.239911 | 5.16E-10 |
| Education | 0.167667 | 0.158416 | 0.999986 |
| Sex | −0.12838 | 0.36527 | 0.981173 |

power, leading to higher cortical excitability, an increased excitation-to-inhibition ratio, and a higher level of neural noise (Trondle et al., 2023). These effects, coupled with decreased network integration (reduced global efficiency and small-worldness) (Javaid et al., 2022; Meunier et al., 2009; Achard and Bullmore, 2007; Onoda and Yamaguchi, 2013), suggests disruptions in local and network communication effectiveness. Age was also associated with a loss of functional specialization (segregation), manifesting as smaller and more local modules across brain networks (Song et al., 2014). Thus, aging may be characterized by an increased asynchronous activity and reduced network integration and segregation.

Better cognition was associated with increased cortical activation, and decreased asynchronous neural activity. Improved cognition predicted enhanced information processing capacity, as reflected in increased alpha power across occipital electrodes (Hindriks and van Putten, 2013; Pfurtscheller and Lopes da Silva, 1999). Better cognition was also associated with an increase in general spiking activity (offset) (Pei et al., 2023; Zhang et al., 2023; Waschke et al., 2021) and a decrease in neural noise (slope) (Smith et al., 2023; Ouyang et al., 2020; Pei et al., 2023) in occipital, temporal, and hippocampal regions. This aligns with previous results showing that aperiodic activity reflects dynamic adjustments of metacognitive states crucial for successful cognitive performance (Zhang et al., 2023). A positive association with whole-brain entropy and a negative with FD and spectral structure confirmed the role of complex dynamics in cognition (Iinuma et al., 2022; Parbat and Chakraborty, 2021). Thus, increased cognitive performance is consistently associated with both local and global dynamics, involving increased cortical activation, enhanced alpha oscillations, and complex brain dynamics.

Fewer years of education correlated with higher individual alpha frequencies in frontal regions and reduced integration and segregation of brain networks. However, these associations were weaker in comparison with other metrics, as reported with fMRI (Raz et al., 2005). While direct assessments of education as a predictor of EEG metrics have been limited in prior studies, previous research including education as a covariate, showed no significant effects on periodic frequency (da Cruz et al., 2020) or graph-theoretic measures (Tan et al., 2019). Similarly, sex did not emerge as the most influential predictor in any model. Sex differences have been observed (Carrier et al., 2001; Pravitha et al., 2005) and not detected in EEG studies (Trondle et al., 2023; Rempe et al., 2023; Gaubert et al., 2019). Our results suggest that sex is a less influential individual predictor, although it influences signals when combined with other demographic or cognitive variables. The impact of education and gender on brain phenotypes should be further investigated by exploring more specific measures capturing population diversity.

Across all models, periodic frequency and graph-theoretic measures demonstrated the highest sensitivity in capturing individual differences. Older age, worse cognition, and being male predicted lower alpha power, while older age and lower education were associated with less integrated and segregated networks. Even when combined with age, education was not found to be an influential predictor, supporting a weak relationship between this factor and brain signals (Raz et al., 2005; da Cruz et al., 2020; Tan et al., 2019). Older age and worse cognition, when combined, are linked to reduced alpha power and increased neural noise, aligning with the neural noise hypothesis of aging (Voytek et al., 2015; Cremer and Zeef, 1987), stating that with increasing age, neural noise rises, and the reliability of neural communication diminishes, contributing to cognitive decline. Therefore, age-related cognitive decline might be attributed to these combined effects, where decreased alpha oscillatory activity allows for more neural noise, which, in turn, disrupts neural communication (Voytek et al., 2015). As complexity and aperiodic components can emerge by intrinsical modulation of brain dynamics, or as a consequence of metabolic or energetic impairments (Medel et al., 2023; Kluger et al., 2023), future studies should investigate the influence of individual differences in demographics and cognition on changes in these metrics.

It is worth noting that some models demonstrated low $R^2$ values ($R^2 < 0.1$); the residuals of these models did not show an approximately normal distribution and exhibited poor fit. However, due to the intrinsic complexity of neuroimaging data and the inherent variability in brain-behavior associations, even models with low $R^2$ can provide valuable insights into the effects among variables. Additionally, the variation in $R^2$ values provide important information about the strongest effects.

### 4.1. Limitations

Several limitations of our study should be acknowledged. Cognitive data were only available for a subsample of participants. Additionally, cognition was assessed using a screening tool. Although the MMSE has been widely used as a reliable measure of general cognitive state (Folstein et al., 1975), it may not fully encompass the spectrum of cognitive abilities. Contrary to prior findings associating graph metrics with cognition (Bullmore and Sporns, 2009; Yu et al., 2021; Stanley et al., 2015), our results indicated that MMSE scores did not possess strong predictive value. Limited performance variability in MMSE scores, with all participants scoring above 24, affects the range and reduces variability. We acknowledge the limitations of the MMSE as a tool for assessing cognition, particularly in healthy populations. However, we

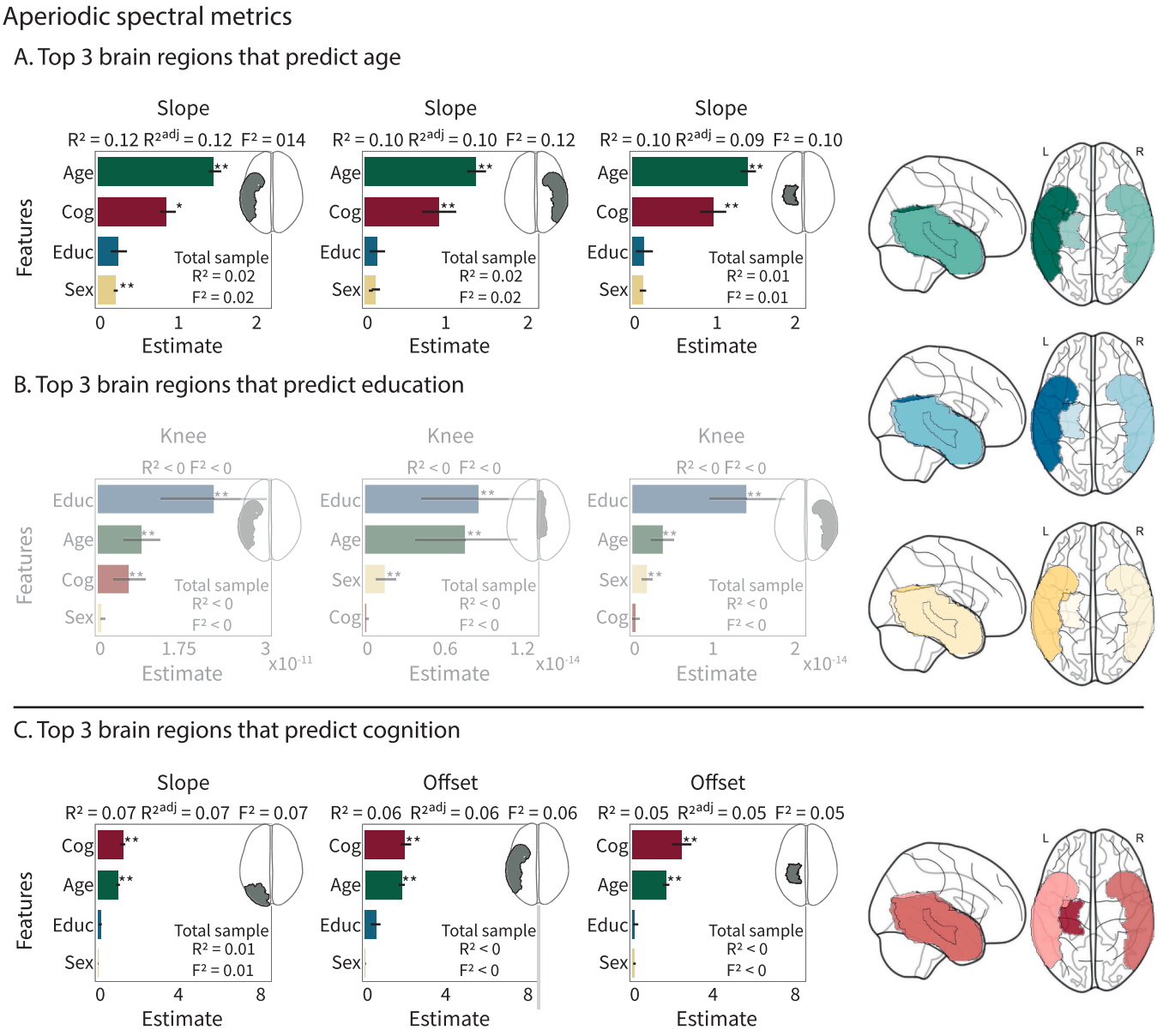


**Fig. 3. Results on the models using aperiodic spectral metrics as outcomes. (A)** The three best models when age was the best-evaluated feature identified age and cognition as the metrics with the highest evaluation, both of which were statistically significant. Education and sex did not reach statistical significance. In the total sample, $R^2$ experienced a decrease, but the models remained statistically significant. **(B)** The models when education was the best-evaluated feature were presented with transparency because none of them were statistically significant. **(C)** The three best models when cognition was the best-evaluated feature had an $R^2$ lower than 0.1, but they were still statistically significant. Education and Sex did not attain statistical significance in any model. In the total sample, the models experienced a significant decrease in $R^2$. The brains in the right column represent the intensity of predictors in the respective brain regions for statistically significant models, for the subsample with cognitive data. The models in hippocampus and temporal regions were the most significant ones. The statistical values for the models with the complete sample are provided within each box.

employed the MMSE because it remains a valuable cognitive screening in both clinical and research settings. Its widespread availability, ease of use, and brevity render it a useful tool for initial cognitive assessment in environments necessitating rapid and accessible evaluations (Creavin et al., 2016). Further assessments should explore the role of individual differences in cognition using more comprehensive measures across various cognitive domains. Moreover, the measure of years of education may not be sufficiently sensitive to capture population diversity in this factor. Future studies should consider incorporating more detailed measures that provide information on the quality and nature of education received by participants. As we did not inquire about gender identities, a factor that can significantly influence diversity among populations, future studies should systematically address individual differences related to gender identities to provide a more comprehensive understanding of the associated brain signatures. Also, although country-level analyses are highly relevant, we included only a limited number of nations with unbalanced sample sizes, thereby reducing the possibilities for cross-country interpretations. Although these effects are beyond the scope of this work, future global approaches with larger, balanced, and more diverse samples should explore country-level effects effectively.

It is also worth noting that the choice of parceling scheme and methodology for defining the ROIs can influence the outcomes. In our study, we opted to employ ROIs for two primary reasons: (i) To mitigate potential effects resulting from employing different electrode configurations and quantities, given the EEG's low spatial resolution and the

**Table 4**
Results for complexity metrics on the subsample with available cognitive data.

| A. Models with cognition as the best evaluated feature | | | |
|---|---|---|---|
| Whole brain (FD), $F = 55.40$, $p < 1e15$, $R^2 = 0.13$, $R^2$ adjusted = 0.13, CI = 0.08, $F^2 = 0.16$ | | | |
| Predictors | **Estimate** | **t value** | **p value** |
| Cognition | −0.42149 | 2.832611 | <1e-15 |
| Age | 0.177473 | 2.26391 | 3.4E-10 |
| Sex | 0.094606 | 2.451106 | 4.67E-12 |
| Education | −0.06247 | 0.497431 | 0.862861 |
| Whole brain (WE), $F = 39.14$, $p < 1e15$, $R^2 = 0.10$, $R^2$ adjusted = 0.10, CI = 0.042, $F^2 = 0.11$ | | | |
| Predictors | **Estimate** | **t value** | **p value** |
| Cognition | 0.468037 | 3.762755 | <1e-15 |
| Sex | −0.07337 | 2.284629 | 1.97E-10 |
| Age | 0.072522 | 1.117352 | 0.02743 |
| Education | 0.018191 | 0.226368 | 0.999692 |
| Left inferior frontal gyrus (spectral structure variation), $F = 36.81$, $p < 1e15$, $R^2 = 0.09$, $R^2$ adjusted = 0.09, CI = 0.04, $F^2 = 0.10$ | | | |
| Predictors | **Estimate** | **t value** | **p value** |
| Cognition | −0.15205 | 3.071085 | <1e-15 |
| Sex | 0.030633 | 2.395504 | 1.67E-11 |
| Education | −0.00804 | 0.24164 | 0.999116 |
| Age | 9.56E-05 | 0.225578 | 0.999868 |

variance in estimation error that arises from using low and high-density electrode configurations. This approach facilitates comparison of results across a broad spectrum of electrode arrangements and quantities. (ii) To reduce the number of regressions. Despite this reduction, we still had to construct a substantial number of models. On the other hand, using ROIs requires finding consistent effects in broad regions, and as our results demonstrate, they displayed robust effects. Future studies using only high-density arrays should explore the impact of spatial variation using finer areas. In adittion, we observed variations in the number of channels across different centers, ranging from 21 to 132 electrodes. To address the potential effects of these variations, we employed a mesh model approach for integrating the electrode layouts (Melnik et al., 2017). We applied spatial normalization to ensure that the EEG inversion process remains unaffected by the number of channels (Prado et al., 2023). This was verified by confirming that the number of channels did not predict the signal quality in the source space. Furthermore, our results were reported with an MNI average brain for source estimation, given that individual MRI data was unavailable. Source space provides more adequate spatial resolution with 64+ channels. Although challenging, source analysis can be efficiently done with low-density electrodes (Nguyen-Danse et al., 2021; Soler et al., 2020; Baroumand et al., 2018). We constructed a regression model to predict signal quality based on the number of channels, which yielded non-significant results, suggesting that the number of channels did not impact the reported associations. We avoided analyzing small regions and focus only on larger effects. However, using the MNI average brain for source estimation with low electrode density represents a limitation. Future studies should conduct further analyses of the impact of the number of channels on source variability and its associations with brain phenotypes.

Moreover, the correlation among the reported outcomes exhibited expected values. Metrics that were spatially close showed high levels of correlation, as did the connectivity metrics. However, the regressions of predictors with the outcomes were independent of the relationships among the outcomes. We opt to use different measures as is typical in the literature (Cesnaite et al., 2023; Zappasodi et al., 2015; Donoghue et al., 2020; Vecchio et al., 2022) and emphasize their individual effects. Finally, we identified collinearity between cognition and education in the sample with cognitive data, while there were no collinearity in the complete sample. Collinearity can cause issues with estimated accuracy, high coefficient variances, interpretation challenges, among others (Snee, 1983). However, our models showed a high level of consistency and precision in their estimates across both samples (sample with cognitive data and the total sample). The results yielded the same effects when employing a collinearity-robust model such as Ridge regression (Tsigler and Bartlett, 2024).

### 4.2. Implications and future directions

Despite the diversity of our sample and the heterogeneity in data acquisition across centers, our results revealed that demographic and cognitive factors robustly predicted EEG modulations. These findings reflect the potential of using more affordable and scalable techniques, such as EEG, for the study of individual differences contributing to diversity and brain signatures. Although we did not include EEG microstates in this work, as it was beyond the scope of our study, previous reports have shown sex-specific changes in microstate dynamics during adolescence as well as at older age (Tomescu et al., 2018). Additionally, changes in microstates have been associated with age, from childhood (Hill et al., 2023) to adulthood (Koenig et al., 2002). As EEG microstates can inform the temporal dynamics of large-scale brain networks across millisecond timescales, future studies should use them to explore the predictive value of demographic and cognitive factors across large and diverse populations. Similarly, given that other complexity metrics like multiscale entropy have shown sensitivity to variations in age (Wang et al., 2016) and cognition (Maturana-Candelas et al., 2019), future research should leverage these tools in large and diverse samples.

Future studies should employ EEG metrics in normative modeling to create brain charts as anchor points for standardized quantification of brain functioning over the lifespan, considering individual differences contributing to population diversity. Normative modeling with neuroimaging measures (Bethlehem et al., 2022; Elad et al., 2021; Di Biase et al., 2023; Rutherford et al., 2022; Habes et al., 2021; Rosenberg et al., 2020) has clarified individual differences in the context of brain development or aging, brain health and disease, and mapping variations across multiple cognitive domains. The development of has brain charts challenged traditional interpretations of case-control differences (Marquand et al., 2016), which become problematic in domains such as neurodegeneration and psychiatry where disorders are diagnosed based on symptoms that overlap between disorders, often yielding heterogeneous clinical groups. As normative modeling does not require categorical partitioning, applying this approach using EEG signals will allow for a more global applicability in parsing heterogeneity and diversity in brain health, psychiatry, and neurodegeneration.

Our findings endorse EEG as a potential tool that, in the future, should be critically incorporated into case-control studies in clinical settings (Rossini et al., 2020). While EEG offers numerous benefits for investigating physiological changes linked to pathology, it often relies on group-level data to identify associations or differences, which limits its utility at the individual diagnostic level. Established methods like MRI, PET, and cerebral spinal fluid analysis offer undeniable value in individual diagnosis; however, they are often expensive and have limited accessibility, particularly in resource-constrained settings. EEG offers complementary accessible tools that can aid in revealing physiological changes linked to early pathology and the risk of dementia (Rossini et al., 2020; Parra, 2022).

### 4.3. Conclusion

Variations in EEG metric typically used in case-control studies are influenced by individual differences in demographics and cognition. Older age, poorer cognition, and being male were associated with reduced alpha power, whereas older age and less education were linked to less integrated and segregated networks. Moreover, older age and worse cognition were linked to reduced alpha power and increased neural noise. Our findings pave the way for the future use of EEG-based brain charts for standardized quantification of brain functioning over the lifespan, considering individual differences contributing to

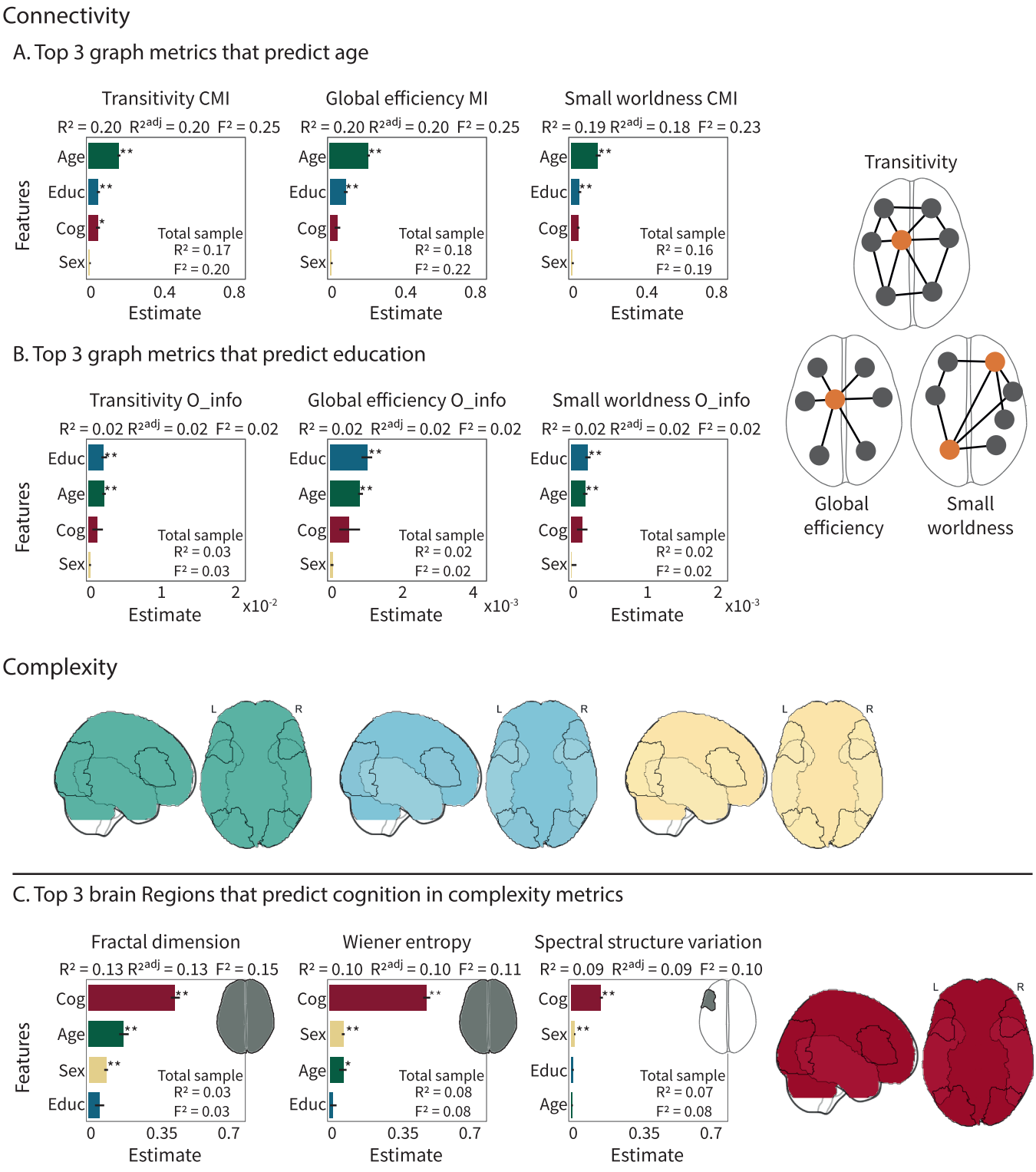


**Fig. 4. Results on the models using connectivity and complexity metrics as outcomes.** In terms of connectivity metrics, cognition never emerged as the best-evaluated feature, whereas in complexity metrics, neither age nor education stood out as the top-rated predictors. **(A)** The three best models when age was the primary feature exhibited significant results with high $R^2$ values and effect sizes for measures of segregation, integration, and small-worldness. Age and education were the best evaluated and significant predictors in the models. In the total sample, the models maintained almost the same performance. **(B)** The three best models when education was the primary feature yielded a low $R^2$ but remained statistically significant. Education and age were the best-evaluated predictors, whereas cognition and sex did not hold significance. **(C)** Results for complexity metrics. The three best models when cognition was the primary feature for predicting connectivity metrics emerged with several complexity metrics: fractal dimension, spectral structure variability, and Wiener entropy. Cognition had a much higher value compared to other predictors. In the total sample, the models significantly decreased $R^2$ values (see values inside the box). Brains in this panel indicate that the most predominant regions were the whole brain, along with the occipital, inferior frontal gyrus, and temporal lobe. These regions prevailed in both hemispheres. The brains to the right of panels **(A)** and **(B)** represent the utilized connectivity metrics for the subsample with cognitive data. The statistical values for the models with the complete sample are provided within each box.

**Table 5**
Results for graph- theoretic measures on the subsample with available cognitive data.

| A. Models with age as the best evaluated feature | | | |
|---|---|---|---|
| Transitivity (CMI), $F = 90.62$, $p < 1e15$, $R^2 = 0.20$, $R^2$ adjusted = 0.20, CI = 0.062, $F^2 = 0.26$] | | | |
| Predictors | **Estimate** | **t value** | **p value** |
| Age | −0.16318 | 5.923662 | <1e-15 |
| Education | −0.06215 | 1.44298 | 0.000756 |
| Cognition | 0.059867 | 1.105595 | 0.032926 |
| Sex | −0.0124 | 0.921539 | 0.138854 |
| Global efficiency (MI), $F = 88.94$, $p < 1e15$, $R^2 = 0.20$, $R^2$ adjusted = 0.20, CI = 0.045, $F^2 = 0.24$ | | | |
| Predictors | **Estimate** | **t value** | **p value** |
| Age | −0.197 | 6.135292 | <1e-15 |
| Education | −0.0807 | 1.563886 | 0.000111 |
| Cognition | 0.037216 | 0.576938 | 0.756623 |
| Sex | −0.00805 | 0.509363 | 0.870492 |
| Small worldness (CMI), $F = 81.90$, $p < 1e15$, $R^2 = 0.19$, $R^2$ adjusted = 0.18, CI = 0.06, $F^2 = 0.23$ | | | |
| Predictors | **Estimate** | **t value** | **p value** |
| Age | −0.14729 | 5.520251 | <1e-15 |
| Education | −0.05611 | 1.346702 | 0.00252 |
| Cognition | 0.050124 | 0.952187 | 0.115618 |
| Sex | −0.01036 | 0.791281 | 0.315885 |
| **B. Models with education as the best evaluated feature** | | | |
| Transitivity (O_info), $F = 8.40$, $p = 0.026$, $R^2 = 0.02$, $R^2$ adjusted = 0.02, CI = 0.04, $F^2 = 0.01$ | | | |
| Predictors | **Estimate** | **t value** | **p value** |
| Education | 0.002819 | 1.238426 | 0.008346 |
| Age | 0.00281 | 1.977057 | 1.33E-07 |
| Cognition | −0.00181 | 0.645702 | 0.717019 |
| Sex | 0.000173 | 0.257998 | 0.999564 |
| Global efficiency (O_info), $F = 8.04$, $p = 0.014$, $R^2 = 0.03$, $R^2$ adjusted = 0.02, CI = 0.04, $F^2 = 0.024$ | | | |
| Predictors | **Estimate** | **t value** | **p value** |
| Education | 0.001219 | 1.355786 | 0.00202 |
| Age | 0.001002 | 1.79685 | 3.16E-06 |
| Cognition | −0.00065 | 0.571754 | 0.848408 |
| Sex | 4.97E-05 | 0.246322 | 0.99862 |
| Small worldness (O_info), $F = 7.30$, $p = 0.017$, $R^2 = 0.02$, $R^2$ adjusted = 0.02, CI = 0.04, $F^2 = 0.02$ | | | |
| Predictors | **Estimate** | **t value** | **p value** |
| Education | 0.000295 | 1.412363 | 0.001037 |
| Age | 0.00025 | 1.921802 | 3.78E-07 |
| Cognition | −0.0002 | 0.758745 | 0.468241 |
| Sex | 1.49E-05 | 0.267985 | 0.998259 |

population diversity. Such an approach will allow for more tailored global models to understanding the variations and diversity in brain health, psychiatry, and neurology.

## CRediT authorship contribution statement

**Hernan Hernandez:** Writing – review & editing, Writing – original draft, Methodology, Investigation, Formal analysis, Conceptualization. **Sandra Baez:** Writing – review & editing, Writing – original draft, Investigation, Formal analysis, Conceptualization. **Vicente Medel:** Writing – review & editing, Supervision, Investigation, Conceptualization. **Sebastian Moguilner:** Writing – review & editing, Methodology, Investigation, Formal analysis, Conceptualization. **Jhosmary Cuadros:** Writing – review & editing, Supervision, Investigation, Data curation. **Hernando Santamaria-Garcia:** Writing – review & editing, Supervision, Investigation, Conceptualization. **Enzo Tagliazucchi:** Writing – review & editing, Supervision, Investigation, Conceptualization. **Pedro A. Valdes-Sosa:** Writing – review & editing, Supervision, Investigation, Conceptualization. **Francisco Lopera:** Writing – review & editing, Supervision, Investigation, Conceptualization. **John Fredy OchoaGómez:** Writing – review & editing, Supervision, Investigation. **Alfredis González-Hernández:** Writing – review & editing, Supervision, Investigation. **Jasmin Bonilla-Santos:** Writing – review & editing, Supervision, Investigation. **Rodrigo A. Gonzalez-Montealegre:** Writing – review & editing, Supervision, Investigation. **Tuba Aktürk:** Writing – review & editing, Supervision, Investigation. **Ebru Yıldırım:** Writing – review & editing, Supervision, Investigation. **Renato Anghinah:** Writing – review & editing, Supervision, Investigation, Data curation. **Agustina Legaz:** Writing – review & editing, Supervision, Investigation, Data curation. **Sol Fittipaldi:** Writing – review & editing, Supervision, Investigation. **Görsev G. Yener:** Writing – review & editing, Supervision, Resources, Investigation, Funding acquisition. **Javier Escudero:** Writing – review & editing, Supervision, Investigation. **Claudio Babiloni:** Writing – review & editing, Supervision, Investigation. **Susanna Lopez:** Writing – review & editing, Supervision, Investigation. **Robert Whelan:** Writing – review & editing, Supervision, Investigation, Conceptualization. **Alberto A Fernández Lucas:** Writing – review & editing, Supervision, Investigation. **Adolfo M. García:** Writing – review & editing, Supervision, Investigation. **David Huepe:** Writing – review & editing, Supervision, Investigation. **Gaetano Di Caterina:** Writing – review & editing, Supervision, Investigation. **Marcio Soto-Añari:** Writing – review & editing, Validation, Investigation. **Agustina Birba:** Writing – review & editing, Supervision, Investigation. **Agustin Sainz-Ballesteros:** Writing – review & editing, Supervision, Investigation. **Carlos Coronel:** Writing – review & editing, Validation, Investigation. **Eduar Herrera:** Writing – review & editing, Supervision, Investigation. **Daniel Abasolo:** Writing – review & editing, Supervision, Investigation. **Kerry Kilborn:** Writing – review & editing, Supervision, Investigation. **Nicolás Rubido:** Writing – review & editing, Supervision, Investigation. **Ruaridh Clark:** Writing – review & editing, Supervision, Investigation. **Ruben Herzog:** Writing – review & editing, Supervision, Investigation. **Deniz Yerlikaya:** Writing – review & editing, Supervision, Investigation. **Bahar Güntekin:** Writing – review & editing, Supervision, Investigation. **Mario A. Parra:** Writing – review & editing, Supervision, Resources, Investigation, Funding acquisition. **Pavel Prado:** Writing – review & editing, Supervision, Investigation. **Agustin Ibanez:** Writing – review & editing, Writing – original draft, Supervision, Methodology, Investigation, Funding acquisition, Conceptualization.

## Declaration of competing interest

none.

## Data availability

Both the data and analysis codes are openly accessible through the following GitHub link https://github.com/euroladbrainlat/Brain-health-in-diverse-setting.

*Acknowledgments*

This work was supported by the Latin American Brain Health Institute (BrainLat) Seed Grant BL-SRGP2020-02 awarded to MAP and AI. AMG is an Atlantic Fellow at the Global Brain Health Institute (GBHI) and is partially supported with funding from the National Institute On Aging of the National Institutes of Health (R01AG075775, 2P01AG019724); ANID (FONDECYT Regular 1210176, 1210195); GBHI, Alzheimer's Association, and Alzheimer's Society (Alzheimer's Association GBHI ALZ UK-22-865742); the Latin American Brain Health Institute (BrainLat), Universidad Adolfo Ibáñez, Santiago, Chile (#BL-SRGP2021-01); Programa Interdisciplinario de Investigación Experimental en Comunicación y Cognición (PIIECC), Facultad de Humanidades, USACH. AI is supported by grants from the MULTI-PARTNER CONSORTIUM TO EXPAND DEMENTIA RESEARCH IN LATIN AMERICA [ReDLat, supported by Fogarty International Center (FIC), National Institutes of Health, National Institutes of Aging (R01 AG057234, R01 AG075775, R01 AG21051, R01 AG083799, CARDS-NIH), Alzheimer's

Association (SG-20-725707), Rainwater Charitable Foundation – The Bluefield project to cure FTD, and Global Brain Health Institute)], USS-FIN-23-FAPE-09, ANID/FONDECYT Regular (1210195 and 1210176 and 1220995); ANID/FONDAP/15150012; ANID/PIA/ANILLOS ACT210096; FONDEF ID20I10152, and ANID/FONDAP 15150012. The contents of this publication are solely the responsibility of the authors and do not represent the official views of these institutions.

## Supplementary materials

Supplementary material associated with this article can be found, in the online version, at doi:10.1016/j.neuroimage.2024.120636.

## References

Achard, S., Bullmore, E., 2007. Efficiency and cost of economical brain functional networks. PLoS. Comput. Biol. 3 (2), e17.
Alladi, S., Hachinski, V., 2018. World dementia: one approach does not fit all. Neurology. 91 (6), 264–270.
Allouh, M.Z., Al Barbarawi, M.M., Ali, H.A., Mustafa, A.G., Alomari, S.O, 2020. Morphometric analysis of the corpus callosum according to age and sex in middle eastern arabs: racial comparisons and clinical correlations to Autism Spectrum Disorder. Front. Syst. Neurosci. 14, 30.
Al Zoubi, O., Ki Wong, C., Kuplicki, R.T., Yeh, H.W., Mayeli, A., Refai, H., et al., 2018. Predicting Age From Brain EEG Signals-A. Mach. Learn. Approach. Front. Aging Neurosci. 10, 184.
Aoki, Y., Ishii, R., Pascual-Marqui, R.D., Canuet, L., Ikeda, S., Hata, M., et al., 2015. Detection of EEG-resting state independent networks by eLORETA-ICA method. Front. Hum. Neurosci. 9, 31.
Aoki, Y., Kazui, H., Pascal-Marqui, R.D., Ishii, R., Yoshiyama, K., Kanemoto, H., et al., 2019a. EEG Resting-State Networks in Dementia with Lewy Bodies Associated with Clinical Symptoms. Neuropsychobiology. 77 (4), 206–218.
Aoki, Y., Kazui, H., Pascual-Marqui, R.D., Ishii, R., Yoshiyama, K., Kanemoto, H., et al., 2019b. EEG resting-state networks responsible for gait disturbance features in idiopathic normal pressure hydrocephalus. Clin. EEG. Neurosci. 50 (3), 210–218.
Aranda, M.P., Kremer, I.N., Hinton, L., Zissimopoulos, J., Whitmer, R.A., Hummel, C.H., et al., 2021. Impact of dementia: health disparities, population trends, care interventions, and economic costs. J. Am. Geriatr. Soc. 69 (7), 1774–1783.
Asadzadeh, S., Yousefi, Rezaii T, Beheshti, S., Delpak, A., Meshgini, S, 2020. A systematic review of EEG source localization techniques and their applications on diagnosis of brain abnormalities. J. Neurosci. Methods 339, 108740.
Babiloni, C., Barry, R.J., Basar, E., Blinowska, K.J., Cichocki, A., Drinkenburg, W., et al., 2020. International federation of clinical neurophysiology (IFCN) - EEG research workgroup: recommendations on frequency and topographic analysis of resting state EEG rhythms. Part 1: applications in clinical research studies. Clin. Neurophysiol. 131 (1), 285–307.
Baez, S., Alladi, S., Ibanez, A., 2023. Global South research is critical for understanding brain health, ageing and dementia. Clin. Transl. Med. 13 (11).
Ballesteros, A.S., Prado, P., Ibanez, A., Perez, J.A.M., Moguilner, S., 2023. A Pipeline for Large-scale Assessments of Dementia EEG Connectivity Across Multicentric Settings. In: Preprints, O (Ed.), A Pipeline for Large-scale Assessments of Dementia EEG Connectivity Across Multicentric Settings. editor.
Baroumand, A.G., van Mierlo, P., Strobbe, G., Pinborg, L.H., Fabricius, M., Rubboli, G., et al., 2018. Automated EEG source imaging: a retrospective, blinded clinical validation study. Clin. Neurophysiol. 129 (11), 2403–2410.
Bassett, D.S., Bullmore, E.T., 2017. Small-World Brain Networks Revisited. Neuroscientist. 23 (5), 499–516.
Bazanova, O.M., Vernon, D., 2014. Interpreting EEG alpha activity. Neurosci. Biobehav. Rev. 44, 94–110.
Benjamini, Y., Hochberg, Y., 1995. Controlling the false discovery rate: a practical and powerful approach to multiple testing. J. R. Stat. Soc.: Series B (Methodological) 57 (1), 289–300.
Bethlehem, R.A.I., Seidlitz, J., White, S.R., Vogel, J.W., Anderson, K.M., Adamson, C., et al., 2022. Brain charts for the human lifespan. Nature 604 (7906), 525–533.
Bigdely-Shamlo, N., Kreutz-Delgado, K., Kothe, C., Makeig, S., 2013. EyeCatch: data-mining over half a million EEG independent components to construct a fully-automated eye-component detector. Annu Int. Conf. IEEe Eng. Med. Biol. Soc. 2013, 5845–5848.
Bigdely-Shamlo, N., Mullen, T., Kothe, C., Su, K.M., Robbins, K.A., 2015. The PREP pipeline: standardized preprocessing for large-scale EEG analysis. Front. Neuroinform. 9, 16.
Bishop, C.M., 2006. Pattern Recognition and Machine Learning. Springer, New York [2006]©2006.
Boncompte, G., Medel, V., Cortínez, L.I., Ossandón, T., 2021. Brain activity complexity has a nonlinear relation to the level of propofol sedation. Br. J. Anaesth. 127 (2), 254–263.
Bullmore, E., Sporns, O., 2009. Complex brain networks: graph theoretical analysis of structural and functional systems. Nat. Rev. Neurosci. 10 (3), 186–198.
Burns T., Rajan R. A mathematical approach to correlating objective spectro-temporal features of environmental sounds with their subjective perceptions2016.
Burns, T., Rajan, R., 2015. Combining complexity measures of EEG data: multiplying measures reveal previously hidden information. F1000Res. 4, 137.
Buzsáki, G., 2006. Rhythms of the Brain. Oxford University Press. https://doi.org/10.1093/acprof:oso/9780195301069.001.0001. Available from.
Carrier, J., Land, S., Buysse, D.J., Kupfer, D.J., Monk, T.H., 2001. The effects of age and gender on sleep EEG power spectral density in the middle years of life (ages 20-60 years old). Psychophysiology. 38 (2), 232–242.
Cebi, M., Babacan, G., Oktem, Tanor O, Gurvit, H, 2020. Discrimination ability of the Short Test of Mental Status (STMS) compared to the Mini Mental State Examination (MMSE) in the spectrum of normal cognition, mild cognitive impairment, and probable Alzheimer's disease dementia: the Turkish standardization study. J. Clin. Exp. Neuropsychol. 42 (5), 450–458.
Cesnaite, E., Steinfath, P., Jamshidi, Idaji M, Stephani, T., Kumral, D., Haufe, S., et al., 2023. Alterations in rhythmic and non-rhythmic resting-state EEG activity and their link to cognition in older age. Neuroimage 268, 119810.
Cohen J. Statistical Power Analysis for the Behavioral Sciences: L. Erlbaum Associates; 1988.
Cole, J.H., Ritchie, S.J., Bastin, M.E., Valdes, Hernandez MC, Munoz Maniega, S., Royle, N., et al., 2018. Brain age predicts mortality. Mol. Psychiatry 23 (5), 1385–1392.
Cover T.M., Thomas J.A. Entropy, relative entropy and mutual information. Elements Inform. Theory. 2nd edition 2005. p. 13–55.
Creavin, S.T., Wisniewski, S., Noel-Storr, A.H., Trevelyan, C.M., Hampton, T., Rayment, D., et al., 2016. Mini-Mental State Examination (MMSE) for the detection of dementia in clinically unevaluated people aged 65 and over in community and primary care populations. Cochrane Database Syst. Rev. 2016 (1), CD011145.
Cremer, R., Zeef, E.J., 1987. What kind of noise increases with age? J. Gerontol. 42 (5), 515–518.
Cruzat, J., Herzog, R., Prado, P., Sanz-Perl, Y., Gonzalez-Gomez, R., Moguilner, S., et al., 2023. Temporal Irreversibility of Large-Scale Brain Dynamics in Alzheimer's Disease. J. Neurosci. 43 (9), 1643–1656.
da Cruz, J.R., Favrod, O., Roinishvili, M., Chkonia, E., Brand, A., Mohr, C., et al., 2020. EEG microstates are a candidate endophenotype for schizophrenia. Nat. Commun. 11 (1), 3089.
Delorme, A., Makeig, S., 2004. EEGLAB: an open source toolbox for analysis of single-trial EEG dynamics including independent component analysis. J. Neurosci. Methods 134 (1), 9–21.
Di Biase, M.A., Tian, Y.E., Bethlehem, R.A.I., Seidlitz, J., Alexander-Bloch, A.F., Yeo, B.T. T., et al., 2023. Mapping human brain charts cross-sectionally and longitudinally. Proc. Natl. Acad. Sci. U. S. A. 120 (20), e2216798120.
Dimitriadis, S.I., 2022. Universal Lifespan Trajectories of Source-Space Information Flow Extracted from Resting-State MEG Data. Brain Sci. 12 (10).
Donoghue, T., Haller, M., Peterson, E.J., Varma, P., Sebastian, P., Gao, R., et al., 2020b. Parameterizing neural power spectra into periodic and aperiodic components. Nat. Neurosci. 23 (12), 1655–1665.
Donoghue, T., Haller, M., Peterson, E.J., Varma, P., Sebastian, P., Gao, R., et al., 2020a. Parameterizing neural power spectra into periodic and aperiodic components. Nat. Neurosci. 23 (12), 1655–U288.
Doppelmayr, M., Klimesch, W., Pachinger, T., Ripper, B., 1998. Individual differences in brain dynamics: important implications for the calculation of event-related band power. Biol. Cybern. 79 (1), 49–57.
Dotson, V.M., Duarte, A., 2020. The importance of diversity in cognitive neuroscience. Ann. N. Y. Acad. Sci. 1464 (1), 181–191.
Elad, D., Cetin-Karayumak, S., Zhang, F., Cho, K.I.K., Lyall, A.E., Seitz-Holland, J., et al., 2021. Improving the predictive potential of diffusion MRI in schizophrenia using normative models-Towards subject-level classification. Hum. Brain Mapp. 42 (14), 4658–4670.
Faul, F., Erdfelder, E., Lang, A.G., G*Power, Buchner A., 2007. 3: a flexible statistical power analysis program for the social, behavioral, and biomedical sciences. Behav. Res. Methods 39 (2), 175–191.
Finnigan, S., Robertson, I.H., 2011. Resting EEG theta power correlates with cognitive performance in healthy older adults. Psychophysiology. 48 (8), 1083–1087.
Fisher, R.A., 1992. Statistical Methods for Research Workers. In: Kotz, S, Johnson, NL (Eds.), Breakthroughs in Statistics: Methodology and Distribution. Springer New York, New York, NY, pp. 66–70.
Fittipaldi, S., Legaz, A., Maito, M., Hernandez, H., Altschuler, F., Canziani, V., et al., 2023. Heterogeneous factors influence social cognition across diverse settings in brain health and age-related diseases. Res. Sq.
Foderaro, G., Isella, V., Mazzone, A., Biglia, E., Di Gangi, M., Pasotti, F., et al., 2022. Brand new norms for a good old test: northern Italy normative study of MiniMental State Examination. Neurol. Sci. 43 (5), 3053–3063.
Folstein, M.F., Folstein, S.E., McHugh, P.R., 1975. "Mini-mental state". A practical method for grading the cognitive state of patients for the clinician. J. Psychiatr. Res. 12 (3), 189–198.
Franzmeier, N., Duering, M., Weiner, M., Dichgans, M., Ewers, M., 2017b. Alzheimer's Disease Neuroimaging I. Left frontal cortex connectivity underlies cognitive reserve in prodromal Alzheimer disease. Neurology. 88 (11), 1054–1061.
Franzmeier, N., Gottler, J., Grimmer, T., Drzezga, A., Araque-Caballero, M.A., Simon-Vermot, L., et al., 2017a. Resting-state connectivity of the left frontal cortex to the default mode and dorsal attention network supports reserve in mild cognitive impairment. Front. Aging Neurosci. 9, 264.
Gaal, Z.A., Boha, R., Stam, C.J., Molnar, M., 2010. Age-dependent features of EEG-reactivity–spectral, complexity, and network characteristics. Neurosci. Lett. 479 (1), 79–84.
Garcia, M.A., Saenz, J., Downer, B., Wong, R., 2018. The role of education in the association between race/ethnicity/nativity, cognitive impairment, and dementia among older adults in the United States. Demogr. Res. 38, 155–168.

Garo-Pascual, M., Gaser, C., Zhang, L., Tohka, J., Medina, M., Strange, B.A., 2023. Brain structure and phenotypic profile of superagers compared with age-matched older adults: a longitudinal analysis from the Vallecas Project. Lancet Healthy. Longev. 4 (8), e374–ee85.
Gaubert, S., Raimondo, F., Houot, M., Corsi, M.C., Naccache, L., Diego, Sitt J, et al., 2019. EEG evidence of compensatory mechanisms in preclinical Alzheimer's disease. Brain 142 (7), 2096–2112.
Gordon, B.A., Rykhlevskaia, E.I., Brumback, C.R., Lee, Y., Elavsky, S., Konopack, J.F., et al., 2008. Neuroanatomical correlates of aging, cardiopulmonary fitness level, and education. Psychophysiology. 45 (5), 825–838.
Górecka, J., Walerjan, P., 2011. Artifacts Extraction from EEG Data Using the Infomax Approach. Biocybern. Biomed. Eng. 31, 59–74.
Grech, R., Cassar, T., Muscat, J., Camilleri, K.P., Fabri, S.G., Zervakis, M., et al., 2008. Review on solving the inverse problem in EEG source analysis. J. Neuroeng. Rehabil. 5, 25.
Greene, A.S., Gao, S., Noble, S., Scheinost, D., Constable, R.T., 2020. How Tasks change whole-brain functional organization to reveal brain-phenotype relationships. Cell Rep. 32 (8), 108066.
Greene, A.S., Shen, X., Noble, S., Horien, C., Hahn, C.A., Arora, J., et al., 2022. Brain-phenotype models fail for individuals who defy sample stereotypes. Nature 609 (7925), 109–118.
Habes, M., Pomponio, R., Shou, H., Doshi, J., Mamourian, E., Erus, G., et al., 2021. The Brain Chart of Aging: machine-learning analytics reveals links between brain aging, white matter disease, amyloid burden, and cognition in the iSTAGING consortium of 10,216 harmonized MR scans. Alzheimers. Dement. 17 (1), 89–102.
Haegens, S., Cousijn, H., Wallis, G., Harrison, P.J., Nobre, A.C, 2014. Inter- and intra-individual variability in alpha peak frequency. Neuroimage 92 (100), 46–55.
Heger, I.S., Deckers, K., Schram, M.T., Stehouwer, C.D.A., Dagnelie, P.C., van der Kallen, C.J.H., et al., 2021. Associations of the Lifestyle for Brain Health Index With Structural Brain Changes and Cognition Results From the Maastricht Study. Neurology. 97 (13), E1300–E1E12.
Hemmati, S., Ahmadlou, M., Gharib, M., Vameghi, R., Sajedi, F., 2013. Down syndrome's brain dynamics: analysis of fractality in resting state. Cogn. Neurodyn. 7 (4), 333–340.
Herzog, R., Rosas, F.E., Whelan, R., Fittipaldi, S., Santamaria-Garcia, H., Cruzat, J., et al., 2022. Genuine high-order interactions in brain networks and neurodegeneration. Neurobiol. Dis. 175, 105918.
Hill, A.T., Bailey, N.W., Zomorrodi, R., Hadas, I., Kirkovski, M., Das, S., et al., 2023. EEG microstates in early-to-middle childhood show associations with age, biological sex, and alpha power. Hum. Brain Mapp. 44 (18), 6484–6498.
Hill, A.T., Clark, G.M., Bigelow, F.J., Lum, J.A.G., Enticott, P.G., 2022. Periodic and aperiodic neural activity displays age-dependent changes across early-to-middle childhood. Dev. Cogn. Neurosci. 54, 101076.
Hinault, T., Baillet, S., Courtney, S.M., 2023. Age-related changes of deep-brain neurophysiological activity. Cereb. Cortex. 33 (7), 3960–3968.
Hindriks, R., van Putten, M.J., 2013. Thalamo-cortical mechanisms underlying changes in amplitude and frequency of human alpha oscillations. Neuroimage 70, 150–163.
Holmes, A.J., Patrick, L.M., 2018. The myth of optimality in clinical neuroscience. Trends. Cogn. Sci. 22 (3), 241–257.
Hu, S., Lai, Y., Valdes-Sosa, P.A., Bringas-Vega, M.L., Yao, D., 2018. How do reference montage and electrodes setup affect the measured scalp EEG potentials? J. Neural Eng. 15 (2), 026013.
Hunt, B.A.E., Wong, S.M., Vandewouw, M.M., Brookes, M.J., Dunkley, B.T., Taylor, M.J., 2019. Spatial and spectral trajectories in typical neurodevelopment from childhood to middle age. Netw. Neurosci. 3 (2), 497–520.
Ibanez, A., Legaz, A., Ruiz-Adame, M., 2023. Addressing the gaps between socioeconomic disparities and biological models of dementia. Brain 146, 3561–3564.
Iinuma, Y., Nobukawa, S., Mizukami, K., Kawaguchi, M., Higashima, M., Tanaka, Y., et al., 2022. Enhanced temporal complexity of EEG signals in older individuals with high cognitive functions. Front. Neurosci. 16, 878495.
Imperatori, L.S., Betta, M., Cecchetti, L., Canales-Johnson, A., Ricciardi, E., Siclari, F., et al., 2019. EEG functional connectivity metrics wPLI and wSMI account for distinct types of brain functional interactions. Sci. Rep. 9 (1), 8894.
Ince, R.A., Giordano, B.L., Kayser, C., Rousselet, G.A., Gross, J., Schyns, P.G., 2017. A statistical framework for neuroimaging data analysis based on mutual information estimated via a gaussian copula. Hum. Brain Mapp. 38 (3), 1541–1573.
Ishii, R., Canuet, L., Aoki, Y., Hata, M., Iwase, M., Ikeda, S., et al., 2017. Healthy and pathological brain aging: from the perspective of oscillations, functional connectivity, and signal complexity. Neuropsychobiology. 75 (4), 151–161.
Javaid, H., Kumarnsit, E., Chatpun, S., 2022. Age-related alterations in EEG network connectivity in healthy aging. Brain Sci. 12 (2).
Jawinski, P., Markett, S., Drewelies, J., Duzel, S., Demuth, I., Steinhagen-Thiessen, E., et al., 2022. Linking Brain Age Gap to Mental and Physical Health in the Berlin Aging Study II. Front. Aging Neurosci. 14, 791222.
Jeong, H.T., Youn, Y.C., Sung, H.H., Kim, S.Y., 2021. Power spectral changes of quantitative eeg in the subjective cognitive decline: comparison of community normal control groups. Neuropsychiatr. Dis. Treat. 17, 2783–2790.
Jokinen, H., Melkas, S., Madureira, S., Verdelho, A., Ferro, J.M., Fazekas, F., et al., 2016. Cognitive reserve moderates long-term cognitive and functional outcome in cerebral small vessel disease. J. Neurol. Neurosurg. Psychiatry 87 (12), 1296–1302.
Jovicich, J., Barkhof, F., Babiloni, C., Herholz, K., Mulert, C., 2019. Harmonization of Neuroimaging Biomarkers For Neurodegenerative diseases: A survey in the Imaging Community of Perceived Barriers and Suggested Actions, 11. Alzheimer's & dementia, (Amsterdam, Netherlands), pp. 69–73.
Kalauzi, A., Bojić, T., Rakić, L., 2009. Extracting complexity waveforms from one-dimensional signals. Nonlinear. Biomed. Phys. 3 (1), 8.
Kida, T., Tanaka, E., Kakigi, R., 2016. Multi-Dimensional Dynamics of Human Electromagnetic Brain Activity. Front. Hum. Neurosci. 9.
Klimesch, W., 1999b. EEG alpha and theta oscillations reflect cognitive and memory performance: a review and analysis. Brain Res. Brain Res. Rev. 29 (2–3), 169–195.
Klimesch, W., 1999a. EEG alpha and theta oscillations reflect cognitive and memory performance: a review and analysis. Brain Res. Rev. 29 (2), 169–195.
Kluger, D.S., Forster, C., Abbasi, O., Chalas, N., Villringer, A., Gross, J., 2023. Modulatory dynamics of periodic and aperiodic activity in respiration-brain coupling. Nat. Commun. 14 (1), 4699.
Kochhann, R., Varela, J.S., Lisboa, C.S.M., Chaves, M.L.F., 2010. The Mini Mental State Examination: review of cutoff points adjusted for schooling in a large Southern Brazilian sample. Dement. Neuropsychol. 4 (1), 35–41.
Koenig, T., Prichep, L., Lehmann, D., Sosa, P.V., Braeker, E., Kleinlogel, H., et al., 2002. Millisecond by millisecond, year by year: normative EEG microstates and developmental stages. Neuroimage 16 (1), 41–48.
Kothe, C.A., Makeig, S., 2013. BCILAB: a platform for brain-computer interface development. J. Neural Eng. 10 (5), 056014.
Krause, D., Folkerts, M., Karch, S., Keeser, D., Chrobok, A.I., Zaudig, M., et al., 2015. Prediction of Treatment outcome in patients with obsessive-compulsive disorder with low-resolution brain electromagnetic tomography: a prospective EEG study. Front. Psychol. 6, 1993.
Lau, Z.J., Pham, T., Chen, S.H.A., Makowski, D., 2022. Brain entropy, fractal dimensions and predictability: a review of complexity measures for EEG in healthy and neuropsychiatric populations. Eur. J. Neurosci. 56 (7), 5047–5069.
Lee, H.Y., Jung, K.I., Yoo, W.K., Ohn, S.H., 2019. Global Synchronization Index as an Indicator for Tracking Cognitive Function Changes in a Traumatic Brain Injury Patient: a Case Report. Ann. Rehabil. Med. 43 (1), 106–110.
Lejko, N., Larabi, D.I., Herrmann, C.S., Aleman, A., Curcic-Blake, B., 2020. Alpha power and functional connectivity in cognitive decline: a systematic review and meta-analysis. J. Alzheimers. Dis. 78 (3), 1047–1088.
Li, X., Ouyang, G., Richards, D.A., 2007. Predictability analysis of absence seizures with permutation entropy. Epilepsy Res. 77 (1), 70–74.
Liao, X., Vasilakos, A.V., He, Y., 2017. Small-world human brain networks: perspectives and challenges. Neurosci. Biobehav. Rev. 77, 286–300.
Livingston, G., Huntley, J., Sommerlad, A., Ames, D., Ballard, C., Banerjee, S., et al., 2020. Dementia prevention, intervention, and care: 2020 report of the Lancet Commission. Lancet. 396 (10248), 413–446.
Manly, B.F.J, 1997. Randomization, Bootstrap and Monte Carlo Methods in Biology, second edition. Taylor & Francis.
Marek, S., Tervo-Clemmens, B., Calabro, F.J., Montez, D.F., Kay, B.P., Hatoum, A.S., et al., 2022. Reproducible brain-wide association studies require thousands of individuals. Nature 603 (7902), 654–660.
Marquand, A.F., Rezek, I., Buitelaar, J., Beckmann, C.F., 2016. Understanding heterogeneity in clinical cohorts using normative models: beyond case-control studies. Biol. Psychiatry 80 (7), 552–561.
Martinez-Canada, P., Perez-Valero, E., Minguillon, J., Pelayo, F., Lopez-Gordo, M.A., Morillas, C., 2023. Combining aperiodic 1/f slopes and brain simulation: an EEG/MEG proxy marker of excitation/inhibition imbalance in Alzheimer's disease. Alzheimers. Dement. (Amst) 15 (3), e12477.
Matshabane, O.P., 2021. Promoting diversity and inclusion in neuroscience and neuroethics. EBioMedicine 67, 103359.
Maturana-Candelas, A., Gomez, C., Poza, J., Pinto, N., Hornero, R., 2019. EEG Characterization of the Alzheimer's Disease Continuum by Means of Multiscale Entropies. Entropy. (Basel) 21 (6).
Mazziotta, J., Toga, A., Evans, A., Fox, P., Lancaster, J., Zilles, K., et al., 2001. A probabilistic atlas and reference system for the human brain: international Consortium for Brain Mapping (ICBM). Philos. Trans. R. Soc. Lond. B Biol. Sci. 356 (1412), 1293–1322.
McBride, J.C., Zhao, X., Munro, N.B., Smith, C.D., Jicha, G.A., Hively, L., et al., 2014. Spectral and complexity analysis of scalp EEG characteristics for mild cognitive impairment and early Alzheimer's disease. Comput. Methods Programs Biomed. 114 (2), 153–163.
Medel, V., Irani, M., Crossley, N., Ossandon, T., Boncompte, G., 2023b. Complexity and 1/f slope jointly reflect brain states. Sci. Rep. 13 (1), 21700.
Medel, V., Irani, M., Crossley, N., Ossandón, T., Boncompte, G., 2023a. Complexity and 1/f slope jointly reflect brain states. Sci. Rep. 13 (1), 21700.
Melnik, A., Legkov, P., Izdebski, K., Kärcher, S.M., Hairston, W.D., Ferris, D.P., et al., 2017. Systems, Subjects, Sessions: to What Extent Do These Factors Influence EEG Data? Front. Hum. Neurosci. 11, 150.
Members, E.C.C., Brayne, C., Ince, P.G., Keage, H.A., McKeith, I.G., Matthews, F.E., et al., 2010. Education, the brain and dementia: neuroprotection or compensation? Brain 133 (Pt 8), 2210–2216.
Merkin, A., Sghirripa, S., Graetz, L., Smith, A.E., Hordacre, B., Harris, R., et al., 2023. Do age-related differences in aperiodic neural activity explain differences in resting EEG alpha? Neurobiol. Aging 121, 78–87.
Meunier, D., Achard, S., Morcom, A., Bullmore, E., 2009. Age-related changes in modular organization of human brain functional networks. Neuroimage 44 (3), 715–723.
Miraglia, F., Vecchio, F., Bramanti, P., Rossini, P.M., 2015. Small-worldness characteristics and its gender relation in specific hemispheric networks. Neuroscience 310, 1–11.
Moretti, D.V., Babiloni, C., Binetti, G., Cassetta, E., Dal Forno, G., Ferreric, F., et al., 2004b. Individual analysis of EEG frequency and band power in mild Alzheimer's disease. Clin. Neurophysiol. 115 (2), 299–308.
Moretti, D.V., Babiloni, C., Binetti, G., Cassetta, E., Dal Forno, G., Ferreric, F., et al., 2004a. Individual analysis of EEG frequency and band power in mild Alzheimer's disease. Clin. Neurophysiol. 115 (2), 299–308.

Mukaetova-Ladinska, E.B., De Lillo, C., Arshad, Q., Subramaniam, H.E., Maltby, J., 2022. Cognitive Assessment of Dementia: the Need for an Inclusive Design Tool. Curr. Alzheimer. Res. 19 (4), 265–273.
Muller, A.C., Guido, S., 2018. Introduction to Machine Learning with Python: a Guide for Data Scientists: o'Reilly Media. Incorporated.
Murty, D., Manikandan, K., Kumar, W.S., Ramesh, R.G., Purokayastha, S., Javali, M., et al., 2020. Gamma oscillations weaken with age in healthy elderly in human EEG. Neuroimage 215, 116826.
Nguyen-Danse, D.A., Singaravelu, S., Chauvigné, L.A.S., Mottaz, A., Allaman, L., Guggisberg, A.G., 2021. Feasibility of reconstructing source functional connectivity with low-density EEG. Brain Topogr. 34 (6), 709–719.
Onoda, K., Yamaguchi, S., 2013. Small-worldness and modularity of the resting-state functional brain network decrease with aging. Neurosci. Lett. 556, 104–108.
Ouyang, C.S., Chiang, C.T., Yang, R.C., Wu, R.C., Lin, L.C., 2020b. Quantitative electroencephalogram analysis of frontal cortex functional changes in patients with migraine. Kaohsiung. J. Med. Sci. 36 (7), 543–551.
Ouyang, G., Hildebrandt, A., Schmitz, F., Herrmann, C.S., 2020a. Decomposing alpha and 1/f brain activities reveals their differential associations with cognitive processing speed. Neuroimage 205, 116304.
Ouyang, G., Li, J., Liu, X., Li, X., 2013. Dynamic characteristics of absence EEG recordings with multiscale permutation entropy analysis. Epilepsy Res. 104 (3), 246–252.
Parbat, D., Chakraborty, M., 2021. A novel methodology to study the cognitive load induced eeg complexity changes: chaos, fractal and entropy based approach. Biomed Signal Proces 64.
Parra, M.A., 2022. Barriers to effective memory assessments for Alzheimer's Disease. J. Alzheimers. Dis. 90 (3), 981–988.
Pascual-Marqui, R.D., 2002. Standardized low-resolution brain electromagnetic tomography (sLORETA): technical details. Methods Find. Exp. Clin. Pharmacol. 24 (Suppl D), 5–12.
Pathania, A., Schreiber, M., Miller, M.W., Euler, M.J., Lohse, K.R., 2021. Exploring the reliability and sensitivity of the EEG power spectrum as a biomarker. Int. J. Psychophysiol. 160, 18–27.
Pei, L., Zhou, X., Leung, F.K.S., Ouyang, G., 2023. Differential associations between scale-free neural dynamics and different levels of cognitive ability. Psychophysiology. 60 (6), e14259.
Pfurtscheller, G., Lopes da Silva, F.H., 1999. Event-related EEG/MEG synchronization and desynchronization: basic principles. Clin. Neurophysiol. 110 (11), 1842–1857.
Pinaya, W.H.L., Scarpazza, C., Garcia-Dias, R., Vieira, S., Baecker, L., FdC, P., et al., 2021. Using normative modelling to detect disease progression in mild cognitive impairment and Alzheimer's disease in a cross-sectional multi-cohort study. Sci. Rep. 11 (1), 15746.
Pion-Tonachini, L., Kreutz-Delgado, K., Makeig, S., 2019. ICLabel: an automated electroencephalographic independent component classifier, dataset, and website. Neuroimage 198, 181–197.
Prado, P., Birba, A., Cruzat, J., Santamaria-Garcia, H., Parra, M., Moguilner, S., et al., 2022. Dementia ConnEEGtome: towards multicentric harmonization of EEG connectivity in neurodegeneration. Int. J. Psychophysiol. 172, 24–38.
Prado, P., Mejia, J.A., Sainz-Ballesteros, A., Birba, A., Moguilner, S., Herzog, R., et al., 2023a. Harmonized multi-metric and multi-centric assessment of EEG source space connectivity for dementia characterization. Alzheimers. Dement. (Amst) 15 (3), e12455.
Prado, P., Mejía, J.A., Sainz-Ballesteros, A., Birba, A., Moguilner, S., Herzog, R., et al., 2023c. Harmonized multi-metric and multi-centric assessment of EEG source space connectivity for dementia characterization. Alzheimers. Dement. (Amst) 15 (3), e12455.
Prado, P., Moguilner, S., Mejia, J.A., Sainz-Ballesteros, A., Otero, M., Birba, A., et al., 2023b. Source space connectomics of neurodegeneration: one-metric approach does not fit all. Neurobiol. Dis. 179, 106047.
Pravitha, R., Sreenivasan, R., Nampoori, V.P., 2005. Complexity analysis of dense array EEG signal reveals sex difference. Int. J. Neurosci. 115 (4), 445–460.
Raz, N., Lindenberger, U., Rodrigue, K.M., Kennedy, K.M., Head, D., Williamson, A., et al., 2005. Regional brain changes in aging healthy adults: general trends, individual differences and modifiers. Cereb. Cortex. 15 (11), 1676–1689.
Rempe, M.P., Ott, L.R., Picci, G., Penhale, S.H., Christopher-Hayes, N.J., Lew, B.J., et al., 2023. Spontaneous cortical dynamics from the first years to the golden years. Proc Natl Acad Sci U S A. 120 (4), e2212776120.
Resende, E.P.F., Llibre, Guerra JJ, Miller, B.L, 2019. Health and Socioeconomic Inequities as Contributors to Brain Health. JAMa Neurol. 76 (6), 633–634.
Rolls, E.T., Joliot, M., Tzourio-Mazoyer, N., 2015. Implementation of a new parcellation of the orbitofrontal cortex in the automated anatomical labeling atlas. Neuroimage 122, 1–5.
Rosenberg, M.D., Scheinost, D., Greene, A.S., Avery, E.W., Kwon, Y.H., Finn, E.S., et al., 2020. Functional connectivity predicts changes in attention observed across minutes, days, and months. Proc. Natl. Acad. Sci. U. S. A 117 (7), 3797–3807.
Rossini, P.M., Di Iorio, R., Vecchio, F., Anfossi, M., Babiloni, C., Bozzali, M., et al., 2020. Early diagnosis of Alzheimer's disease: the role of biomarkers including advanced EEG signal analysis. Report from the IFCN-sponsored panel of experts. Clin. Neurophysiol. 131 (6), 1287–1310.
Rossini, P.M., Rossi, S., Babiloni, C., Polich, J., 2007. Clinical neurophysiology of aging brain: from normal aging to neurodegeneration. Prog. Neurobiol. 83 (6), 375–400.
Rubinov, M., Sporns, O., 2010. Complex network measures of brain connectivity: uses and interpretations. Neuroimage 52 (3), 1059–1069.
Rutherford, S., Fraza, C., Dinga, R., Kia, S.M., Wolfers, T., Zabihi, M., et al., 2022. Charting brain growth and aging at high spatial precision. Elife 11.
Santamaria-Garcia, H., Sainz-Ballesteros, A., Hernandez, H., Moguilner, S., Maito, M., Ochoa-Rosales, C., et al., 2023. Factors associated with healthy aging in Latin American populations. Nat. Med. 29 (9), 2248–2258.
Sarasso, S., Casali, A.G., Casarotto, S., Rosanova, M., Sinigaglia, C., Massimini, M., 2021. Consciousness and complexity: a consilience of evidence. Neuroscience of Consciousness niab023.
Schliebs, R., Arendt, T., 2011. The cholinergic system in aging and neuronal degeneration. Behav. Brain Res. 221 (2), 555–563.
Schreckenberger, M., Lange-Asschenfeldt, C., Lochmann, M., Mann, K., Siessmeier, T., Buchholz, H.G., et al., 2004. The thalamus as the generator and modulator of EEG alpha rhythm: a combined PET/EEG study with lorazepam challenge in humans. Neuroimage 22 (2), 637–644.
Seker, M., Ozbek, Y., Yener, G., Ozerdem, M.S., 2021. Complexity of EEG Dynamics for Early Diagnosis of Alzheimer's Disease Using Permutation Entropy Neuromarker. Comput. Methods Programs Biomed. 206, 106116.
Selya, A.S., Rose, J.S., Dierker, L.C., Hedeker, D., Mermelstein, R.J., 2012. A practical guide to calculating Cohen's f(2), a Measure of Local Effect Size, from PROC MIXED. Front. Psychol. 3, 111.
Senner, N.R., Conklin, J.R., Piersma, T., 1814. An ontogenetic perspective on individual differences. Proc. Biol. Sci. 282, 2015.
Shumbayawonda, E., Tosun, P.D., Fernandez, A., Hughes, M.P., Abasolo, D., 2018. Complexity changes in brain activity in healthy ageing: a permutation lempel-ziv complexity study of magnetoencephalograms. Entropy. (Basel) 20 (7).
Singh, N.C., 2011. Measuring the 'complexity' of sound. Pramana 77 (5), 811–816.
Smith, A.E., Chau, A., Greaves, D., Keage, H.A.D., Feuerriegel, D., 2023. Resting EEG power spectra across middle to late life: associations with age, cognition, APOE-varepsilon4 carriage, and cardiometabolic burden. Neurobiol. Aging 130, 93–102.
Smits, F.M., Porcaro, C., Cottone, C., Cancelli, A., Rossini, P.M., Tecchio, F., 2016. Electroencephalographic Fractal Dimension in Healthy Ageing and Alzheimer's Disease. PLoS. One 11 (2), e0149587.
Snee, R., 1983. Regression diagnostics: identifying influential data and sources of collinearity. J. Qual. Technol. 15, 149–153.
Soler, A., Muñoz-Gutiérrez, P.A., Bueno-López, M., Giraldo, E., Molinas, M, 2020. Low-Density EEG for neural activity reconstruction using multivariate empirical mode decomposition. Front. Neurosci. 14, 175.
Song, J., Birn, R.M., Boly, M., Meier, T.B., Nair, V.A., Meyerand, M.E., et al., 2014. Age-related reorganizational changes in modularity and functional connectivity of human brain networks. Brain Connect. 4 (9), 662–676.
Stacey, J.E., Crook-Rumsey, M., Sumich, A., Howard, C.J., Crawford, T., Livne, K., et al., 2021. Age differences in resting state EEG and their relation to eye movements and cognitive performance. Neuropsychologia 157, 107887.
Stanley, M.L., Simpson, S.L., Dagenbach, D., Lyday, R.G., Burdette, J.H., Laurienti, P.J., 2015. Changes in brain network efficiency and working memory performance in aging. PLoS. One 10 (4), e0123950.
Stier, C., Braun, C., Focke, N.K., 2023. Adult lifespan trajectories of neuromagnetic signals and interrelations with cortical thickness. Neuroimage 278, 120275.
Sun, J., Wang, B., Niu, Y., Tan, Y., Fan, C., Zhang, N., et al., 2020. Complexity Analysis of EEG, MEG, and fMRI in Mild Cognitive Impairment and Alzheimer's Disease: a Review. Entropy. (Basel) 22 (2).
Tan, Y., Chen, J., Liao, W., Qian, Z., 2019. Brain function network and young adult smokers: a graph theory analysis study. Front. Psychiatry 10, 590.
Tang, A.S., Oskotsky, T., Havaldar, S., Mantyh, W.G., Bicak, M., Solsberg, C.W., et al., 2022. Deep phenotyping of Alzheimer's disease leveraging electronic medical records identifies sex-specific clinical associations. Nat. Commun. 13 (1), 675.
Tomescu, M.I., Rihs, T.A., Rochas, V., Hardmeier, M., Britz, J., Allali, G., et al., 2018. From swing to cane: sex differences of EEG resting-state temporal patterns during maturation and aging. Dev. Cogn. Neurosci. 31, 58–66.
Tononi, G., Sporns, O., Edelman, G.M., 1994. A measure for brain complexity: relating functional segregation and integration in the nervous system. Proc. Natl. Acad. Sci. 91 (11), 5033–5037.
Trammell, J.P., MacRae, P.G., Davis, G., Bergstedt, D., Anderson, A.E., 2017. The relationship of cognitive performance and the theta-alpha power ratio is age-dependent: an eeg study of short term memory and reasoning during task and resting-state in healthy young and old adults. Front. Aging Neurosci. 9, 364.
Trondle, M., Popov, T., Pedroni, A., Pfeiffer, C., Baranczuk-Turska, Z., Langer, N., 2023. Decomposing age effects in EEG alpha power. Cortex 161, 116–144.
Tsigler, A., Bartlett, P.L., 2024. Benign overfitting in ridge regression. J. Mach. Learn. Res. 24 (1), 123.
Turner, C., Baylan, S., Bracco, M., Cruz, G., Hanzal, S., Keime, M., et al., 2023. Developmental changes in individual alpha frequency: recording EEG data during public engagement events. Imaging Neurosci (Camb) 1, 1–14.
Valdes-Sosa, P.A., Galan-Garcia, L., Bosch-Bayard, J., Bringas-Vega, M.L., Aubert-Vazquez, E., Rodriguez-Gil, I., et al., 2021. The Cuban Human Brain Mapping Project, a young and middle age population-based EEG, MRI, and cognition dataset. Sci. Data 8 (1), 45.
Valsdóttir, V., Magnúsdóttir, B.B., Chang, M.L., Sigurdsson, S., Gudnason, V., Launer, L. J., et al., 2022. Cognition and brain health among older adults in Iceland: the AGES-Reykjavik study. Geroscience 44 (6), 2785–2800.
van Nifterick, A.M., Mulder, D., Duineveld, D.J., Diachenko, M., Scheltens, P., Stam, C.J., et al., 2023. Resting-state oscillations reveal disturbed excitation-inhibition ratio in Alzheimer's disease patients. Sci. Rep. 13 (1), 7419.
Varela, F., Lachaux, J.P., Rodriguez, E., Martinerie, J., 2001. The brainweb: phase synchronization and large-scale integration. Nat. Rev. Neurosci. 2 (4), 229–239.
Vecchio, F., Miraglia, F., Alu, F., Judica, E., Cotelli, M., Pellicciari, M.C., et al., 2022. Human brain networks in physiological and pathological aging: reproducibility of

electroencephalogram graph theoretical analysis in cortical connectivity. Brain Connect. 12 (1), 41–51.
Verdi, S., Kia, S.M., Schott, J.M., Marquand, A., Cole, J.H., 2022. Mapping individualised patterns of atrophy in Alzheimer's disease using neuroanatomical normative models. Alzheimers. Dement. 18 (56).
Voytek, B., Kramer, M.A., Case, J., Lepage, K.Q., Tempesta, Z.R., Knight, R.T., et al., 2015. Age-Related Changes in 1/f Neural Electrophysiological Noise. J. Neurosci. 35 (38), 13257–13265.
Walsh, S., Merrick, R., Brayne, C., 2022. The relevance of social and commercial determinants for neurological health. Lancet Neurol. 21 (12), 1151–1160.
Wang, H., McIntosh, A.R., Kovacevic, N., Karachalios, M., Protzner, A.B., 2016. Age-related Multiscale Changes in Brain Signal Variability in Pre-task versus Post-task Resting-state EEG. J. Cogn. Neurosci. 28 (7), 971–984.
Wang, R., Wang, J., Yu, H., Wei, X., Yang, C., Deng, B, 2015. Power spectral density and coherence analysis of Alzheimer's EEG. Cogn. Neurodyn. 9 (3), 291–304.
Waschke, L., Donoghue, T., Fiedler, L., Smith, S., Garrett, D.D., Voytek, B., et al., 2021. Modality-specific tracking of attention and sensory statistics in the human electrophysiological spectral exponent. Elife 10.
Wilkinson, C.L., Pierce, L.J., Sideridis, G., Wade, M., Nelson, C.A., 2023. Associations between EEG trajectories, family income, and cognitive abilities over the first two years of life. Dev. Cogn. Neurosci. 61, 101260.
Wolfers, T., Beckmann, C.F., Hoogman, M., Buitelaar, J.K., Franke, B., Marquand, A.F., 2020. Individual differences v. the average patient: mapping the heterogeneity in ADHD using normative models. Psychol. Med. 50 (2), 314–323.
Yan, J., Li, T., Wang, H., Huang, H., Wan, J., Nho, K., et al., 2015. Cortical surface biomarkers for predicting cognitive outcomes using group l2,1 norm. Neurobiol. Aging 36 (Suppl 1), S185–S193.
Yu, M., Sporns, O., Saykin, A.J., 2021. Author Correction: the human connectome in Alzheimer disease - relationship to biomarkers and genetics. Nat. Rev. Neurol. 17 (9), 592.
Zappasodi, F., Marzetti, L., Olejarczyk, E., Tecchio, F., Pizzella, V., 2015. Age-related changes in electroencephalographic signal complexity. PLoS One. 10 (11), e0141995.
Zhang, C., Stock, A.K., Muckschel, M., Hommel, B., Beste, C., 2023. Aperiodic neural activity reflects metacontrol. Cereb. Cortex. 33 (12), 7941–7951.
Zhao, L., Zhang, Y., Yu, X., Wu, H., Wang, L., Li, F., et al., 2023. Quantitative signal quality assessment for large-scale continuous scalp electroencephalography from a big data perspective. Physiol. Meas. 44 (3).